Journal of Photochemistry and Photobiology C: Photochemistry Reviews 18 (2014) 71–90

Contents lists available at ScienceDirect

Journal of Photochemistry and Photobiology C: Photochemistry Reviews

journal homepage: www.elsevier.com/locate/jphotochemrev

Review

Genesis of rare molecules using light-induced reactions of matrix-isolated tetrazoles

L.M.T. Frija[a,*], M.L.S. Cristiano[b], A. Gómez-Zavaglia[c,d], I. Reva[c], R. Fausto[c]

[a] Research Institute for Medicines and Pharmaceutical Sciences (iMed.UL), Faculty of Pharmacy, University of Lisbon, Av. Prof. Gama Pinto, 1649-003 Lisbon, Portugal
[b] CCMAR and Department of Chemistry and Pharmacy, F.C.T, University of Algarve, Campus de Gambelas, 8005-039 Faro, Portugal
[c] Department of Chemistry, University of Coimbra, 3004-535, Portugal
[d] Centro de Investigación y Desarrollo en Criotecnología de Alimentos (Conicet La Plata, UNLP), RA-1900, Argentina

ARTICLE INFO

Article history:
Received 8 June 2013
Received in revised form 6 September 2013
Accepted 20 September 2013
Available online 1 October 2013

Keywords:
Tetrazole
Photochemistry
Matrix-isolation
Rare molecules
IR spectroscopy

ABSTRACT

Tetrazoles exhibit a very rich photochemistry, strongly influenced by the nature of substituents in the tetrazolic ring. Photolysis of representative tetrazoles trapped in a rigid environment of solidified noble gases at cryogenic temperatures (usually argon at 10–15 K) results in photofragmentation of the monomeric species with a wide range of exit channels. Since the obtained fragments are generally confined to the matrix cage where they are formed, no subsequent cross-reactions involving species resulting from photolysis can occur, strongly reducing the number of possible photoproducts in comparison with gas phase or solution studies. These conditions introduce a useful simplification for the interpretation of the reaction mechanisms and enable spectroscopic characterization of novel and/or highly reactive molecules. In this review, we provide an updated report on the photolysis of matrix-isolated tetrazoles, focusing on the scope and usefulness of this methodology for generation of rare molecules and investigation of photocleavage pathways. Special emphasis is placed on mechanistic interpretations and characterization of rare molecules and on the relevance of conformation and tautomerism on the photochemistry of the studied compounds.

Contents

* Corresponding author. Fax: +351 21 7946476.
E-mail address: lfrija@ff.ul.pt (L.M.T. Frija).

1389-5567/$20.00
http://dx.doi.org/10.1016/j.jphotochemrev.2013.09.001

Luís M.T. Frija received his degree in Chemistry from the University of Algarve (Portugal) in 2001 and his Ph.D. in Chemistry from the same university in 2008 (M. Lurdes S. Cristiano). Part of the studies he performed during his Ph.D. program were developed in the University of Coimbra (Laboratory for Molecular Cryospectroscopy and Biospectroscopy (LMCB), Department of Chemistry) in the research group of Professor Rui Fausto. His research interests were initially mainly devoted to the design and synthesis of heteroaromatic compounds, such as tetrazoles and benzisothiazoles, of biological and/or pharmacological interest and to the study of their photoreactivity and spectroscopic properties. He worked for two years (2009–2010) as post-doctoral research fellow at the Instituto Superior Técnico-Technical University of Lisbon (C.A.M. Afonso lab.). In 2011, he moved to Faculty of Pharmacy-Lisbon University as post-doctoral fellow and he is working on the development of novel and efficient protocols for synthetic transformations of Portuguese natural resources derived from *Cistus ladaniferus* and *Olea europaea* L.

Maria Lurdes Santos Cristiano obtained her Ph.D. in Chemistry at the University of Liverpool in 1994 under the supervision or professor Robert A.W. Johnstone. After, she had a short post-doctoral fellowship at the Faculty of Medicine, University of Liverpool, where she worked in the oncology research unit led by Professor Hilmar Warenius. She is currently associate professor with habilitation at the Department of Chemistry and Pharmacy of the University of Algarve and the scientist in charge of the Group of Organic Reactivity and Medicinal Chemistry at the Centre of Marine Sciences, CCMAR, member of the associate laboratory Centre for Marine and Environmental Research, CIMAR. Her research interests range from physical organic chemistry and organic reactivity to medicinal chemistry.

Andrea Gómez-Zavaglia obtained her degree in Biochemistry from Buenos Aires University (Argentina, 1993) and received her Ph.D. in Sciences at National University of La Plata (Argentina, 2000). After post-doctoral grants in Buenos Aires, Germany and Portugal, she became a Member of the Research Career from the Argentinean National Research Council (Conicet) as Assistant (2004–2006), Adjunct (2006–2012) and Independent Researcher (2012). She has strong cooperations with research groups and enterprises from more than 10 different countries. She participated in 33 funded projects (leading 16 of them), including the coordination of two multilateral networks. Her scientific interests lie in vibrational spectroscopy (FTIR and Raman), both at a fundamental and applied level, from the isolated molecules to cells. More recently, she is focusing her activity on the application of vibrational spectroscopy to food microbiology, and more specifically to lactic acid bacteria and probiotics.

Igor Reva graduated in Biophysics, with honours, from the Kharkov State University (Ukraine). Upon graduation he worked at the Institute for Low Temperature Physics & Engineering (ILTPE), a major research centre of the National Academy of Sciences of Ukraine (in Kharkov), where he completed, in 1995, Ph.D. degree in Thermophysics and Molecular Physics. In 1997–1998, Igor Reva was awarded a post-doctoral fellowship of the Alexander von Humboldt Foundation and moved to Germany, Max-Planck-Institute (MPI) for Radiation Chemistry (Mülheim a.d. Ruhr), then MPI for Nuclear Physics (Heidelberg). In 1999, he joined the Centre of Chemistry at the University of Coimbra, first as a post-doctoral fellow, and subsequently as a researcher. In 2010, the degree of Habilitation in Chemistry was conferred on Igor Reva by the University of Coimbra, in Molecular Spectroscopy. His research interests are molecular structure, conformational dynamics, tautomerism, vibrational properties, thermochemistry and photochemistry of molecular systems.

Rui Fausto obtained is Ph.D. in Molecular Spectroscopy at the University of Coimbra in 1988. After completing his Ph.D., he had a short post-doctoral fellowship at the National Research Council of Canada, Ottawa, where he worked in Professor Paul R. Carey's research group on Raman and resonance Raman spectroscopies of protein substrates. He is currently Full Professor at the Department of Chemistry of the University of Coimbra and the scientist in charge of the Laboratory for Molecular Cryospectroscopy and Biospectroscopy (LMCB) of the Coimbra Chemistry Research Center. His research interests range from spectroscopy and solid-state photochemistry to chemical imaging, theoretical and computational chemistry and hot-vibrational chemistry.

1. Introduction

The chemistry of tetrazole and its derivatives remains a topic of intense research. The wide interest in this class of compounds stems mainly from their potential and important applications in major areas such as medicine [1], agriculture [2], automobile industry [3], imaging technology [4], coordination chemistry [5] and as high energy materials [6]. In drug design and development, 5-substituted tetrazoles are mostly used as a bioisosteric replacement for the carboxylic acid moiety [1] and the 1,5-disubstituted tetrazole ring is known as an excellent mimic for the *cis*-amide bond [7].

Tetrazoles are also interesting molecules from a structural point of view. Hydrogen atoms directly bound to the tetrazole ring are labile and may give rise to different tautomers, their relative populations depending on the chemical environment. Unsubstituted tetrazole (CN_4H_2) occurs exclusively as the 1*H*-tautomer in the crystalline phase and mostly as the 2*H*-tautomer in the gas phase (~90% of the total population at 90 °C). In solution, both tautomers coexist, with the population of the most polar 1*H*-form increasing with the polarity of the solvent [8–12]. The infrared spectrum of tetrazole (CN_4H_2) isolated in solid argon (T = 10 K) was investigated in one of our previous studies, showing essentially the expected signature of the 2*H*-tetrazole tautomer [13]. The amount of the 1*H*-tautomer in the matrix was found to be *ca.* 10% of that of the most abundant form. That study has solved a long-term controversy regarding the existence of the 1*H*-tautomer of tetrazole in the gas phase [13–16]. In the case of substituted tetrazoles, tautomerism may also involve substituent groups, as was found, for instance, in the case of 1-methyl-tetrazol-5-thione and 2-methyl-tetrazol-5-amine [17,18].

The photoreactivity of tetrazoles has been widely investigated, in solution and in the rigid environment of solid matrices, resulting in a wealth of information that unraveled the potential of tetrazoles as precursors of a wide variety of new scaffolds through photolysis [17–27]. The major factor contributing to the observed range and versatility in photochemical pathways for tetrazoles is the possibility of tautomerism. In general, the presence of labile hydrogen atoms (either directly linked to the tetrazole ring or belonging to the tetrazole substituents) is a source of complexity in photochemical reactions, generally opening additional primary channels or enabling secondary photochemical reactions, concomitantly with the dominant primary photoprocesses, and thus interfering with selectivity and product control [17–19,27–30].

When substituents are linked to the tetrazole ring, the photochemistry of the molecule can also be influenced by their nature and conformational flexibility, which may favor or exclude certain reaction channels, determining the nature and relative amount of the final photoproducts [17,23].

The photochemistry of tetrazoles in solution has been reviewed recently [31]. However, regarding the photochemistry of matrix-isolated tetrazoles, a wide range of information is available but data are dispersed, prompting the need for a comprehensive review.

Matrix isolation is a technique where gaseous atoms or molecules are commonly trapped in an environment of solidified noble gases at temperatures close to absolute zero (matrices can also be built from other gases; essentially inert, like N_2, or even reactive like O_2, for instance) [32–36]. Under these conditions, intramolecular rearrangements are inhibited for any process with an activation barrier larger than a few kJ mol^{-1}. In addition, because the matrix rigidity prevents diffusion of the sample, in general bimolecular reactions are also suppressed. In the matrix, the lifetime of unstable or usually short-lived species can then be increased allowing for detailed structural investigations using conventional spectroscopic techniques [32].

A further advantage of this methodology is that the technique of detection can easily be adapted to the problem under investigation, due to the spectroscopic transparency of the host gas. Vibrational spectroscopy, in particular, becomes a very powerful tool for studies of the structure and reactivity of moderate-size organic molecules (up to 30–35 atoms) when combined with low temperature matrix isolation. Infrared spectroscopy provides direct data on frequencies and intensities of characteristic absorptions of the isolated species, and matrix isolation facilitates obtaining this information, due to the high resolution of infrared matrix spectra and high sensitivity of the method. In the spectra of matrix-isolated compounds, the effect of inhomogeneous band broadening nearly vanishes in comparison with the condensed phase and, unlike for the gaseous state, the fine rotational structure is, in general, completely absent. Besides, unlike for solutions, the effect of the environment on the structure of the molecules under investigation is generally negligible [35]. These factors result in a unique narrowing of bands in vibrational spectra (down to a few tenths of cm^{-1}), which makes possible to detect band shifts of a few wavenumbers that are characteristic for the finest changes of sample's structure. Moreover, because the inert matrix most of times only slightly affects the structure of the isolated molecules it is possible to compare directly matrix experimental results and theoretically calculated spectra, which are commonly obtained for the single molecule *in vacuo*.

One of the most important advantages of matrix isolation spectroscopy is the possibility of following photochemical reactions unambiguously. For a matrix isolated compound, *in situ* photolysis enables selective introduction of energy in the molecule under study, controlling the range of possible rearrangements of the isolated species. Thus, a wide range of intramolecular changes, up to molecule decomposition and formation of new entities, can be studied. In addition, contrarily to what occurs in the gas phase or in solution, where a multitude of possible photochemical reaction pathways leading to different products can be observed, in a matrix the processes are cage-confined (molecular diffusion is inhibited), and therefore a useful simplification to the photochemical reactivity is obtained. For instance, if photofragmentation of a matrix-isolated species occurs, the obtained fragments generally stay in the matrix cage where they are produced. Then, no subsequent cross-reactions involving species resulting from photolysis of different reactant molecules can occur, reducing the number of possible photoproducts in comparison with gas phase or solution studies and thereby facilitating the interpretation of reaction mechanisms.

The matrix-isolation technique, coupled with infrared spectroscopy, has been used for many years to study the photochemistry of several families of molecules with biological or industrial relevance. Among them, tetrazoles have been considered in great detail. The photochemistry of matrix-isolated unsubstituted tetrazole was studied for the first time by Maier et al. [19]. Our recent studies on tetrazole derivatives provided a general pattern of reactivity for this family upon UV irradiation [17,18,22–27]. Besides, the observation of a number of relatively unusual or highly reactive molecules, formed from photolysis of the studied tetrazoles, such as antiaromatic azirines, azides, isocyanates or isothiocyanates, the matrix-isolation approach led, in some cases, to the first spectroscopic characterization of some of these species.

In the following sections of this review, an overview of the photochemistry of matrix-isolated tetrazoles is presented. Special emphasis is put on the potential and interest of this class of compounds as starting materials for light-induced formation of rare chemical species, and on the relevance of conformation and tautomerism for the photochemical reactivity of the studied compounds.

2. Photochemistry of matrix-isolated tetrazoles: an effective tool to generate and characterize rare molecules

2.1. Unsubstituted tetrazole

The photochemistry of matrix-isolated unsubstituted tetrazole was studied for the first time by Maier et al. [19]. Upon photolysis with the 193 nm emission line of an ArF laser, rapid photocleavage of tetrazole was observed, leading to extrusion of N_2 and formation of several different photoproducts, including nitrilimine, carbodiimide, diazomethane, an NCH···NH complex and cyanamide (Scheme 1) [19]. The use of different excitation wavelengths, allowed the accumulation of cyanamide and carbodiimide as final products. That study also delivered the first vibrational signature of matrix-isolated nitrilimine [19].

2.2. 1-(Tetrazol-5-yl)ethanol (TE)

Recently, 1-(tetrazol-5-yl)ethanol (TE) has assumed an important role in the synthesis of tetrazole-saccharinate-type nitrogen ligands [37]. Our recent matrix isolation study of TE allowed a detailed investigation of the structure of the compound [26]. Furthermore, it appears as a representative example of the power of this technique in the investigation of tautomer-selective photochemistry. Indeed, 1-(tetrazol-5-yl)ethanol presents two different tautomeric forms, which are stabilized by different types of intramolecular hydrogen bonds (NH···O or OH···N) (Fig. 1).

Remarkably, these non-covalent interactions were found to be relevant to the different photochemical behavior of the tautomers in an argon matrix.

Both 1*H* and 2*H* tautomers can give rise to different conformational isomers. In the case of tautomer 1*H*, the low barriers separating different conformers allow only the observation of the most stable form, since the higher energy forms convert into the most stable one during deposition of the matrix (this phenomenon is known as

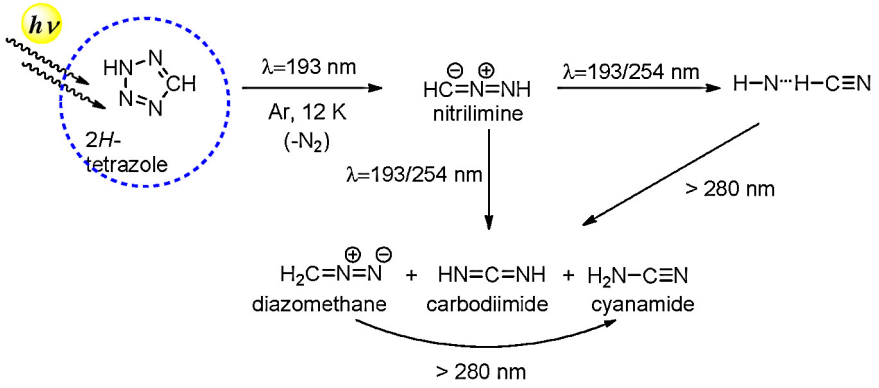

Scheme 1. Photodecomposition of matrix-isolated unsubstituted tetrazole.

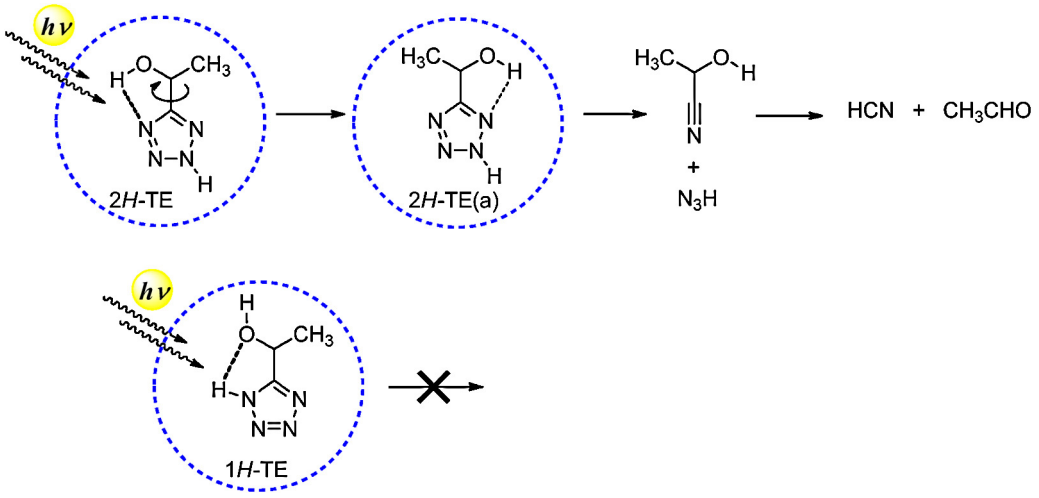

Scheme 2. Photochemical reactions observed for 1-(tetrazole-5-yl)ethanol (TE) isolated in solid argon (30 K) upon irradiation with UV (λ > 200 nm) light.

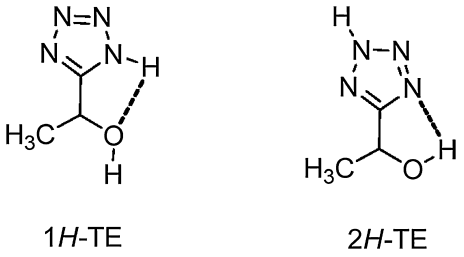

Fig. 1. Tautomeric forms of TE. The dashed lines represent intramolecular hydrogen bonds.

conformational cooling and has been studied in detail in our laboratory) [38–42]. Thus, at 30 K, only two species can be isolated in a solid argon matrix: the most stable forms of 1*H* and 2*H* tautomers. This allowed the observation of a tautomer selective photochemistry, with the 2*H*-tautomeric form undergoing prompt unimolecular decomposition upon irradiation at λ > 200 nm to produce azide and 2-hydroxypropanenitrile, while the 1*H*-tautomer remained photostable (Scheme 2). For the 1*H*-tautomer, photo-induced ring-cleavage requires simultaneous cleavage of the intramolecular H-bond connecting the tetrazole hydrogen to the oxygen atom of the substituent (Scheme 2), which appears to preclude the reaction. In the case of 2*H* tautomer there are low energy conformers that can be easily accessed from the lowest energy conformer in which cleavage of the intramolecular H-bond is not required during the ring-opening reaction. In this case, the ring-opening reaction is then much easier, since the two molecular fragments resulting primarily from the reaction are not linked by any H-bond (Scheme 2).

2.3. 5-Methoxy-1-phenyl-1H-tetrazole (5MPT)

Upon UV irradiation (λ > 235 nm), 5MPT was found to react through two fragmentation pathways (see Scheme 3): (a) N_2 elimination, with production of the antiaromatic 3-methoxy-1-phenyl-1*H*-diazirine (MPD), which was observed experimentally for the first time during our studies [23] and (b) ring-opening, leading to phenylazide and methylcyanate. The latter compound was found to quickly convert to its more stable isomer methyl-isocyanate, in keeping with previous studies [43–46]. Phenylazide further eliminated molecular nitrogen to give phenylnitrene that underwent subsequent ring expansion to

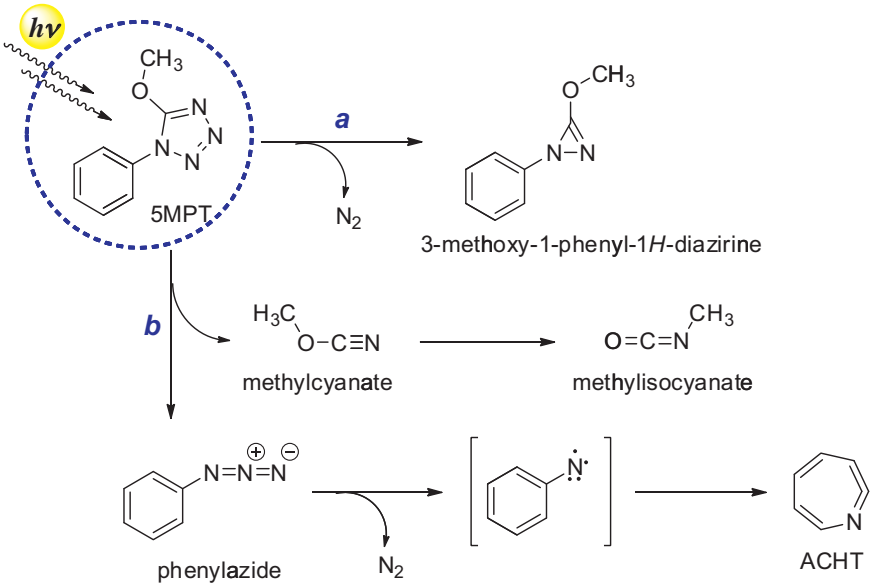

Scheme 3. Photochemical reactions observed for 5-methoxy-1-phenyl-1*H*-tetrazole (5MPT) isolated in solid argon upon irradiation with UV (λ > 235 nm) light.

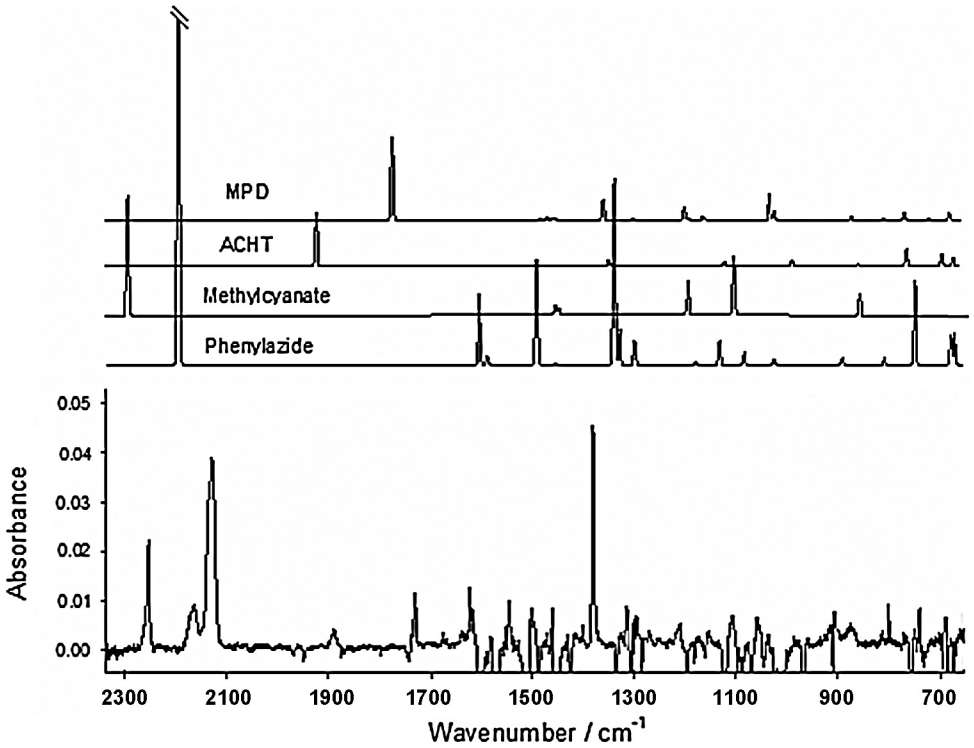

Fig. 2. Bottom: Changes in infrared spectrum of 5MPT trapped in an argon matrix induced by UV (λ > 235 nm) irradiation (spectrum of UV-irradiated (80 min) sample minus spectrum of freshly deposited matrix). Upper frames: B3LYP/6–311++G(d,p) calculated spectra of the observed photoproducts. In the theoretical spectra, intensities were scaled by different factors, in order to better simulate the experimental spectrum presented in the figure.
Reproduced from [23] with permission.

form the seven-membered ring 1-aza-1,2,4,6-cycloheptatetraene (ACHT), which is unambiguously identified by the observation of its characteristic IR band at *ca.* 1913 cm^{-1} (Fig. 2). Identification of phenylazide was straightforward, since the vibrational spectrum of matrix-isolated phenylazide is well-known [28,47,48].

In 5MPT, both observed photoprocesses involve the cleavage of the (N-3)—(N-4) bond. In channel a (Scheme 3), the cleavage of the (N-1)—(N-2) bond occurs in addition. Channel b, which was found to correspond to the preferred reaction channel [23], also implies disruption of the (C-5)—(N-1) bond (Scheme 3). According to DFT(B3LYP)/6–311++G(d,p) calculations performed on 5MPT, these are the three longest bonds in the tetrazole ring (calculated lengths are longer than 135.5 pm) [23]. In turn, the (N-2)—(N-3) and (C-5)—(N-4) bonds were calculated to be considerably shorter (128.0 and 131.3 pm, respectively). Hence, the bonds that are cleft in the photochemical reactions correspond to the weaker bonds which are formally single bonds.

2.4. 5-Ethoxy-1-phenyl-1H-tetrazole (5EPT)

5-Ethoxy-1-phenyl-1*H*-tetrazole (5EPT) differs from 5MPT in the length of the alkyl substituent. The photochemistry of these two molecules was expected to be similar but the increased conformational flexibility brought by the ethoxy group of 5EPT appeared as a source of complexity in the analysis of the experimental data. Indeed, 5EPT possesses 3 conformational isomers, which were predicted by DFT(B3LYP)/6–311++G(d,p) calculations [25] to have relative energies within the 0–3 kJ mol^{-1} range and, then, are all significantly populated in the gas phase prior to deposition. Fortunately, these conformers are separated by low energy barriers (less than 4 kJ mol^{-1}) on the ground-state potential energy surface and, during deposition of the matrix, the higher energy forms relax to the most stable conformer. Hence, only the most stable conformer of 5EPT remains trapped in the as-deposited matrix. This conformer has the ethyl group placed nearly in the plane of the tetrazole ring and as far away as possible from the phenyl group. The dihedral angle between the two rings (phenyl and tetrazole) was calculated to be *ca.* 30° [25].

UV irradiation (λ > 235 nm) of matrix-isolated 5EPT gives rise to different primary photochemical reactions, which are equivalent to those observed for 5MPT: (a) N_2 elimination, leading to production of the anti-aromatic 3-ethoxy-1-phenyl-1*H*-diazirine (EPD), a photoproduct observed and spectroscopically characterized for the first time [25] and (b) tetrazole ring-opening, leading to ethylcyanate and phenylazide (as found for the experiments on 5MPT, phenylazide was also shown to subsequently release N_2, forming phenylnitrene that later rearranges to ACHT). Like in the case of 5MPT, only formally single bonds are cleft in the photoinduced reactions of 5EPT and the pathway leading to ethylcyanate and phenylazide prevails.

The photoproducts diazirine and ethylcyanate possess more than one low energy conformational state but, in the photolysed matrix, were both observed to exist in a single conformation (the *trans* isomer, where the C—O—C—C dihedral is *ca.* 180°; see Fig. 3). Ethylcyanate has one intramolecular degree of freedom, corresponding to the internal rotation around the central (NC)O—C_2H_5 bond, which may result in the existence of different conformers (*trans* and *gauche*). However, DFT(B3LYP)/6–311++G(d,p) calculations indicate that the energy barriers separating the less stable *gauche* conformers from the conformational ground state are very low (less than 4 kJ mol^{-1} [25]). Then, similarly to the matrix-isolated reactant (5EPT), the photochemically obtained ethylcyanate can also undergo conformational cooling upon its production, justifying the sole observation in the irradiated matrices of the most stable *trans* conformer. Three conformers separated by low intramolecular energy barriers (less than 3 kJ mol^{-1}) were also predicted by the DFT(B3LYP)/6–311++G(d,p) calculations for EPD. Again, conformational cooling leads to exclusive observation

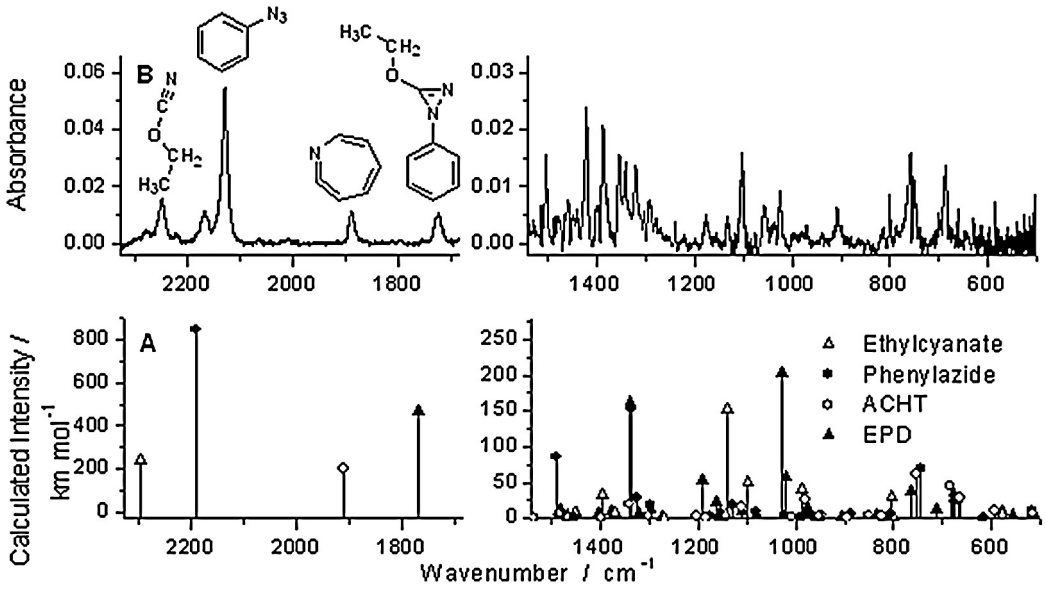

Fig. 3. (A) DFT(B3LYP)/6−311++G(d,p) calculated spectra of the observed photoproducts of 5EPT (scaled with a uniform factor of 0.978). (B) Extracted spectrum of the photoproducts formed after 60 min of UV-irradiation (λ > 235 nm) of 5EPT trapped in an Ar matrix. The extracted spectrum was obtained by subtraction of the scaled spectrum of non-irradiated matrix from the spectrum of irradiated sample. The scaling factor was chosen so that the absorptions due to the originally deposited compound (5EPT) were nullified.
Adapted from [25] with permission.

of the most stable conformer in the 5EPT photolysed matrix. One shall point out that these results demonstrate convincingly that, after their photochemical generation in a low temperature matrix, molecules may undergo efficient conformational cooling to their most stable conformers, since energy dissipation upon returning to the ground state leads to local heating of the matrix, thus facilitating conformational relaxation.

It is also interesting to mention that ethylcyanate is known to isomerize readily at room or higher temperatures to ethylisocyanate [49] and the process is believed to be autocatalyzed [49,50]. Because of its instability, ethylcyanate can only be stored at low temperature and its application in chemical reactions requires its generation *in situ* prior to use [49–52]. For the same reason, this compound had not been the subject of previous detailed experimental structural or vibrational studies and was only characterized in some detail in our investigation [25]. No evidence of isomerization of ethylcyanate to ethylisocyanate was found in our study, indicating that, under matrix-isolation conditions (at temperatures of ~15 K) ethylcyanate is thermally stable and also photostable (λ > 235 nm).

The detailed investigation of the photochemistry of matrix-isolated 5-alkoxytetrazoles (5MPT and 5EPT) [23,25] was instrumental for the interpretation of photochemical pathways of other tetrazole derivatives that exhibit much more complex patterns of photoreactivity, for instance in cases where substitution enables tautomerism involving the tetrazole ring, as described below [18,22,24].

2.5. 2-Methyl-2H-tetrazol-5-amine (2MTA)

When the substituent at the tetrazole ring carbon atom is an amino or imino group, photolysis can result in production of small C-, N- and H-containing molecules of important astrophysical and/or industrial interest (*e.g.*, CN_2H_2, CN_3H or CNH_3 isomers). Thus, investigation of the photochemistry of 2-methyl-2*H*-tetrazol-5-amine (2MTA) was especially challenging. To avoid the increased complexity introduced by the presence of a labile hydrogen atom at the tetrazole ring, 2-methyl-2*H*-tetrazol-5-amine (2MTA) was selected as a simple prototype molecule having the adequate characteristics for studying the photochemistry of amino/imino containing tetrazoles and their photoproducts as well as their structural and vibrational properties.

2MTA may exist in different tautomeric forms (Fig. 4). The possibility of hydrogen shift from the amino group to three different positions of the tetrazole ring leads to three possible pairs of tautomers bearing an imine (or aminide) NH substituent at the position 5 [17]. Taking as reference the atom numbering of the tetrazole ring in 2MTA, the hydrogen involved in the tautomeric rearrangement can occupy positions 1, 3 and 4 of the ring. In the first case tautomerism leads to the imine species, 2-methyl-1,2-dihydro-5*H*-tetrazol-5-imine (structures C in Fig. 4), which can exist in two different conformations, depending on the orientation of the hydrogen atom in the imino group at position 5 [17]. The remaining two cases lead to mesoionic-type structures,

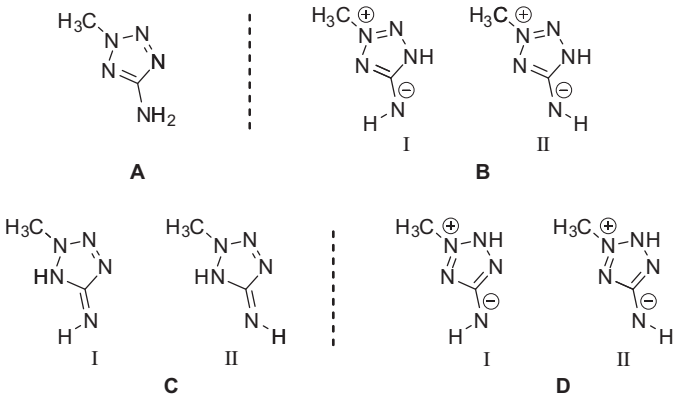

Fig. 4. Structures of 2-methyl-2*H*-tetrazol-5-amine (A) and of its imine (aminide) tautomers: 3-methyl-1*H*-tetrazol-3-ium-5-aminide (B), 2-methyl-1,2-dihydro-5*H*-tetrazol-5-imine (C) and 2-methyl-3*H*-tetrazol-2-ium-5-aminide (D). In the case of the aminide tautomers, the placements of the charges on atoms correspond to one of the possible canonic forms for the mesoionic structures, which were also used to name the compound.

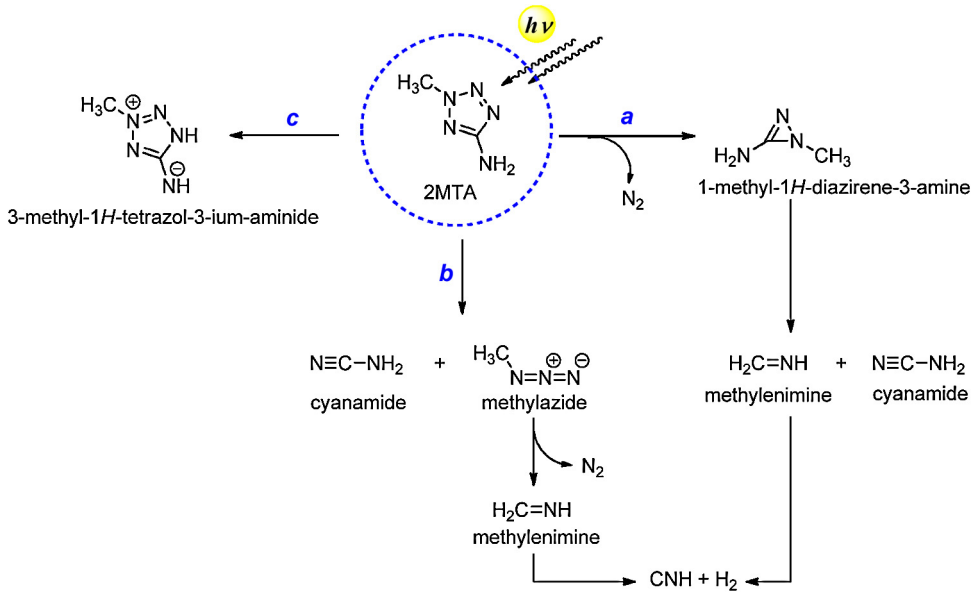

Scheme 4. Photochemical reactions observed for 2-methyl-2*H*-tetrazol-5-amine isolated in solid argon upon irradiation with UV (λ > 235 nm) light.

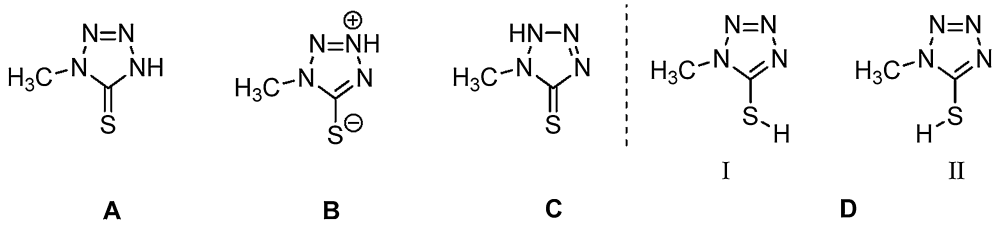

Fig. 5. Tautomers of 5-mercapto-1-methyltetrazole: (A) 1-methyl-1,4-dihydro-5*H*-tetrazol-5-thione, (B) 1-methyl-1*H*-tetrazol-3-ium-5-thiolate; (C) 1-methyl-1,2-dihydro-5*H*-tetrazol-5-thione, (D) 1-methyl-1*H*-tetrazol-5-thiol (two conformers).

2-methyl-3*H*-tetrazol-2-ium-5-aminide (Fig. 4, structure D) and 3-methyl-1*H*-tetrazol-3-ium-5-aminide (Fig. 4, structure B), respectively, that may also exist in two different stable conformations [17].

The experimental spectrum of 2MTA isolated in an argon matrix fits well the spectrum of tautomer A calculated at the DFT(B3LYP)/6−311++G(d,p) level of theory and no evidence of presence of any of the imine (aminide) tautomers was found. This observation is in agreement with the theoretically predicted relative energies of tautomers B, C, D: all of them are less stable than tautomer A by more than 100 kJ mol^{-1} and are not populated in the gas phase [17].

In situ UV irradiation (λ > 235 nm) of matrix-isolated 2MTA induces three main primary photochemical processes. Two of them correspond to the prototype reactions found for other tetrazoles, *viz*, (a) N_2 elimination, with production of 1-methyl-1*H*-diazirine-3-amine, and (b) ring cleavage leading to production of methyl azide and cyanamide. The third observed reaction [pathway (c); Scheme 4] was tautomerization of 2MTA to mesoionic 3-methyl-1*H*-tetrazol-3-ium-5-aminide (tautomer B, Fig. 4) *via* [1,3]-hydrogen shift.

The photoproduced aminide tautomer B(I) is the lowest energy imine/aminide tautomer of 2MTA and, among the six possible imine/aminide tautomers it is one of the two forms that can be directly produced from 2MTA as a result of an energetically accessible hydrogen-shift (see Fig. 4). The other is conformer C(II) of 2-methyl-1,2-dihydro-5*H*-tetrazol-5-imine, which was not identified as contributing to the spectra of the irradiated matrix (this form is less stable than B(I) by *ca.* 20 kJ mol^{-1} and has a non-planar structure, then requiring a more important rearrangement of the matrix to be produced from 2MTA [17]). Once formed, the photoproduced aminide form stays stable in the matrix, since it can be comparatively less photoreactive than 2MTA because the two pathways similar to (a) and (b) would require an additional hydrogen atom migration.

Following the primary photo rearrangements, secondary reactions were observed, leading to spectroscopic identification of methylenimine and hydrogen isocyanide (CNH) [17]. As it can be easily recognized in Scheme 4, these secondary reactions were also facilitated by the presence of labile hydrogen atoms in the primary photoproducts.

2.6. 5-Mercapto-1-methyltetrazole (MTT)

As observed for the 2MTA molecule, tautomerism was expected to be relevant in 5-mercapto-1-methyltetrazole (1-methyl-1*H*-tetrazole-5-thiol; MTT). In this case, tautomerism may be seen as mainly determined by the possibility of the sulphur atom bound to C-5 to adopt the thione or the thiol form (Fig. 5).

The 5-mercapto tautomer D (1-methyl-1*H*-tetrazol-5-thiol) may adopt two different conformers, I and II. Form I, where the methyl group and sulfhydryl hydrogen atom are oriented to opposite sides, is more stable [18]. There are also two 5-thione tautomers, which differ in the position of the tetrazole-ring hydrogen atom (see Fig. 5). The most stable thione tautomer A (1-methyl-1,4-dihydro-5*H*-tetrazol-5-thione) corresponds to the global minimum

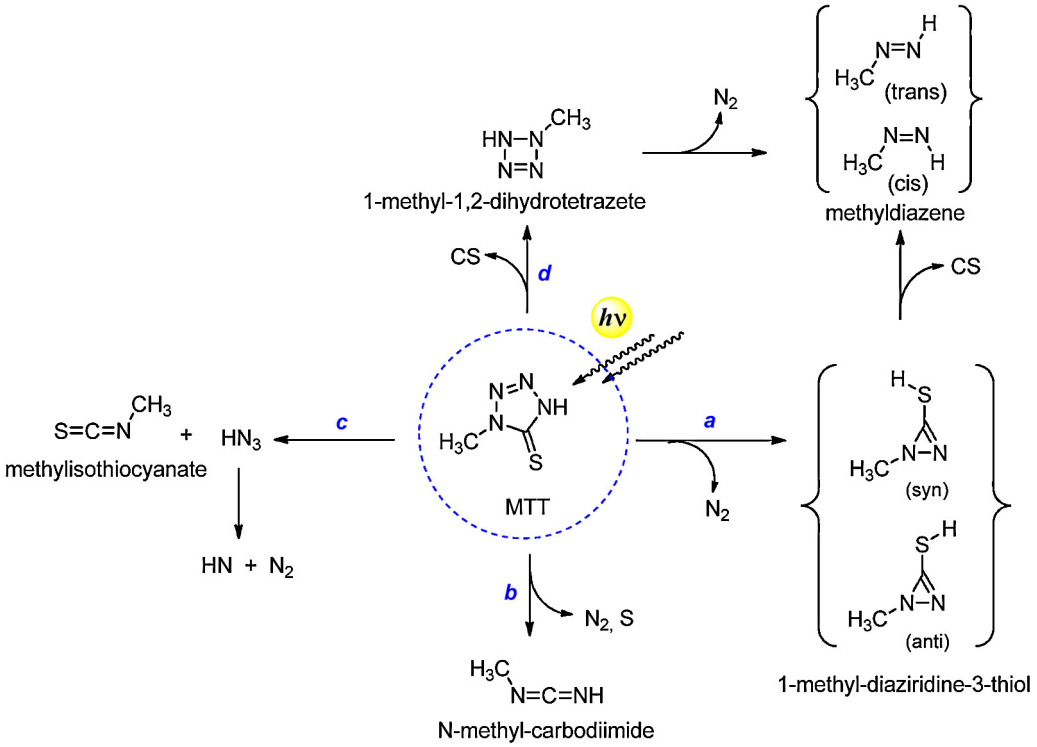

Scheme 5. Photochemical reactions observed for 5-mercapto-1-methyltetrazole isolated in solid argon upon irradiation with UV (λ > 235 nm) light.

of the molecule in the gas phase and is considerably more stable than all other species [thiol tautomer D-I is the second most stable form and has a relative energy of 32.5 kJ mol^{-1}, calculated at the DFT(B3LYP)/6−311++G(d,p)] [18].

As expected from the predicted relative stability of all the possible tautomers of MTT, only the most stable form (1-methyl-1,4-dihydro-5*H*-tetrazol-5-thione) was found in the as-deposited argon matrices. This was clearly demonstrated by the pretty good agreement between the observed infrared spectrum of the as-deposited argon matrix of MTT and that calculated at the DFT(B3LYP)/6−311++G(d,p) level of theory for thione tautomer A [18].

Scheme 5 depicts the proposed reaction pathways for the observed photochemistry of MTT upon irradiation at λ > 235 nm. In general terms, the observed photochemistry of MTT follows closely those observed for other tetrazoles, in particular 2MTA [17] and 1-phenyl-tetrazolone [18]. Nevertheless, the presence of the sulphur atom in the molecule opens additional reaction pathways. Indeed, in MTT molecular nitrogen can be eliminated by two different ways in a primary photolytic step: (a) alone, with simultaneous production of 1-methyl-1*H*-diazirine-3-thiol (MDT, which is produced in two different conformers), and (b) together with atomic sulphur, leading to production of N-methyl-carbodiimide. Pathway (a) is similar to the reaction of 2MTA leading to formation of 1-methyl-1*H*-diazirine-3-amine (see Scheme 4), whereas pathway (b) has no counterpart in the photochemistry of MTT. In addition to the above reactions, MTT can also undergo (c) ring cleavage leading to production of methyl isothiocyanate and azide and (d) elimination of carbon monosulphide leading to production of 1-methyl-1,2-tetrazete (which then eliminates N_2 to form methyl diazene) [18].

Another pathway can also be postulated, involving cleavage of the (C-5)-(N-1) and (N-3)-(N-4) bonds and leading to methyl azide and HNCS, in a similar way to what succeeds for 2MTA. However, despite this pathway could not be discarded in a definitive way, no clear experimental evidence of its occurrence in the present case could be found.

Fig. 6 shows the spectra of matrix-isolated MTT before and after irradiation, in the 2300–1500 cm^{-1} region, where characteristic bands of the photoproducts were observed [18] as well as the calculated spectra of the photoproducts in the same spectral region. The dependence of the experimental spectra on the time of irradiation clearly reveals two types of variation patterns of band intensities: some bands increase in intensity mostly during the first 20 min of irradiation and decrease upon prolonged irradiation (group A bands, 1850–1700 cm^{-1} range), while intensity of other bands (group B, 2250–2050 cm^{-1} range) increases during the whole time of irradiation. Observation of bands of type A clearly indicates that there are primary photoproducts, which undergo secondary reactions. These bands were identified as belonging to 1-methyl-1*H*-diazirine conformers, which undergo secondary photolysis to methyldiazene (with elimination of CS; see Scheme 5). Bands of type B are due to the other photoproducts and were assigned based on results of theoretical calculations of the infrared spectra of the postulated reaction products [18].

It is interesting to note that MTT is a rather reactive tetrazole, under the experimental conditions used, when submitted to UV irradiation (λ > 235 nm). In fact, the bands due to MTT reduce to *ca.* 60% of their initial intensity after the first 20 min of irradiation and to less than 1% after 100 min of irradiation, *i.e.*, MTT almost totally converts into other species after 100 min of irradiation. It is also worth mentioning that at the end of the irradiation process, the *total* intensity of the spectrum was found to be considerably weaker (less than 30% of the initial total absorbance) than that of the as-deposited matrix. This result clearly demonstrates that some of the final products absorb only weakly in the infrared or do not absorb at all (among them, N_2 and S are certainly the dominant species; see Scheme 5). The high observed photoreactivity is in keeping with the widespread usage of tetrazole thiones in imaging systems, namely as stabilizers in photography [53], as deep-UV resists

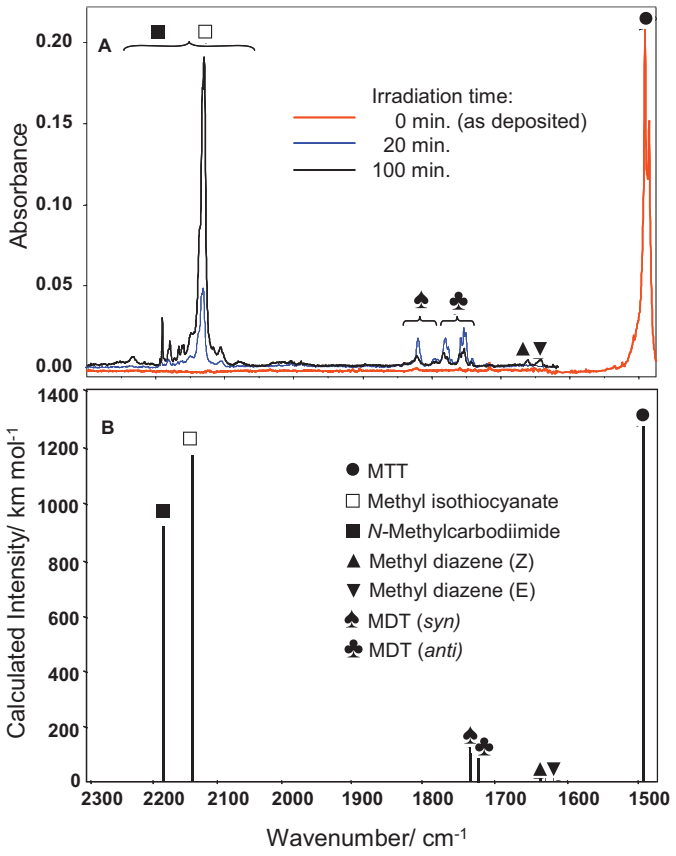

Fig. 6. (A) Infrared spectra (2300–1500 cm^{-1} region) of MTT along the irradiation ($\lambda > 235$ nm) process. (B) DFT(B3LYP)/6−311++G(d,p) calculated spectra for MTT and most of the observed photoproducts (among the identified photoproducts, only CS and HN do not absorb in the spectral region shown in the figure). The intensity of the calculated band of MTT was multiplied by 7, in order to approximately preserve the relative band intensities in the experimental and calculated spectra shown in the figure.

Adapted from [18] with permission.

in photolithographic applications [54] and as photoremovable capping agents in the semiconductor photocatalytic industry [55].

2.7. 1-Phenyl-tetrazolone (PT)

1-Phenyl-tetrazolone (PT) is another tetrazole derivative showing tautomerism. It can exist in five tautomeric forms: two keto tautomers, one mesoionic olate form and two hydroxy conformers (Fig. 7). 1-Phenyl-1,4-dihydro-5*H*-tetrazol-5-one (keto tautomer "A" in Fig. 7) was predicted to be considerably more stable than all the remaining species, due to the existence in this tautomer of more favorable interactions between the phenyl hydrogen atoms *ortho* to the tetrazole ring and the N-2 and carbonyl oxygen atoms [22]. Because of the much greater stability of the "A" tautomer of PT, this is the only species populated in the gas phase at room temperature. Then, tautomer "A" is the unique species initially present in the matrix-isolated PT. This fact strongly simplifies the subsequent photochemical experiments and interpretation of the results.

Compared to 5MPT and 5EPT, the photochemistry of 1-phenyl-tetrazolone (PT) is rather complex. The main observed photoreactions induced by UV light ($\lambda > 235$ nm) in matrix-isolated PT are summarized in Scheme 6. They are: (a) extrusion of molecular nitrogen, giving 1-phenyl-diaziridin-3-one; (b) elimination of HNCO with production of phenylazide; (c) tetrazole ring-opening, leading to phenylisocyanate and azide; and (d) loss of CO, leading to the final production of phenyldiazene and N_2, with all probability occurring via the phenyltetrazete intermediate.

Pathway ***a***, leading to the production of 1-phenyl-diaziridin-3-one, is similar to pathway ***a*** in 5MPT and 5EPT. The photoproduced diaziridinone adopts two different conformers, which were characterized for the first time in our study [22]. Theoretical calculations indicated that the conformer where the phenyl group and the diaziridinone-ring hydrogen atom are *trans* to each other is more stable by 14.5 kJ mol^{-1} than the one where these groups are *cis* to each other. The most intense bands of the diaziridinone isomers correspond to the νC═O and νC—N antisymmetric stretching vibrations and one of the phenyl ring out-of-plane bending modes (γC—H ring 1). All the bands corresponding to these vibrations were identified in the IR spectra of the photolysed matrix [conformer *trans*: 1931.9/1926.0/1877.8/1874.3 cm^{-1} (site-split Fermi resonance doublets resulting from interaction of νC═O with the first overtone of νC—N, see Fig. 8), 964.5/962.8 (νC—N) and 771.0 cm^{-1} (γC—H ring 1); calculated values: 1931.2, 945.5 and 756.2 cm^{-1}; conformer *cis*: 1913.1/1899.4/1865.8/1862.7 (Fig. 8), 924.0/922.8 and 695.3 cm^{-1}, respectively; calculated values: 1921.2, 910.0 and 694.2 cm^{-1}].

The bands due to the diaziridinone are relatively easy to identify, because their intensity increased only during the first stages of irradiation (*i.e.*, until *ca.* 30 min of irradiation). Subsequent irradiation led to a decrease of intensity of these bands, which was accompanied by the appearance in the spectra of new bands (and subsequent progressive growth) that could be assigned to secondary photoproducts resulting from photolysis of the diaziridinone. Two different pathways could be postulated for photodegradation of the diaziridinone, the first one yielding phenyldiazene (in two different conformers) plus CO, and the second one leading to production of phenylnitrene and isocyanic acid. The phenylnitrene underwent the usual subsequent ring expansion to ACHT [16,47,48,56–58], which gives rise to the characteristic bands observed at 1894.2 and 1889.8 cm^{-1} [56,57]. These bands grew mostly at later stages of irradiation (see Fig. 8).

Pathway ***b*** leads to production of phenylazide and isocyanic acid (HNCO) and is similar to pathway ***b*** in 5MPT and 5EPT. The experimental identification of isocyanic acid was complicated because the most intense bands of this compound are nearly coincident with bands due to other photoproducts, in particular phenylisocyanate, which is formed in pathway ***c*** and is one of the major observed photoproducts. Nevertheless, bands assigned to HNCO

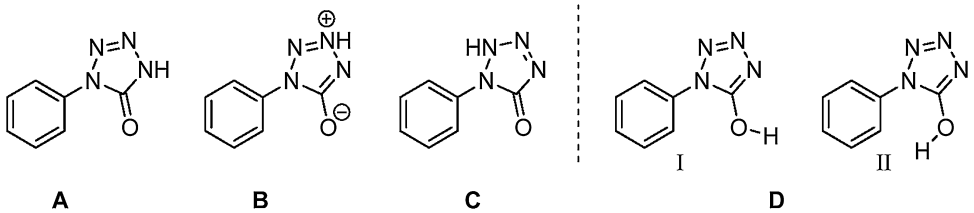

Fig. 7. Tautomers of 1-phenyltetrazolone (PT). (A) 1-phenyl-1,4-dihydro-5*H*-tetrazol-5-one; (B) 1-phenyl-1*H*-tetrazol-3-ium-5-olate; (C) 1-phenyl-1,2-dihydro-5*H*-tetrazol-5-one; (D) 1-phenyl-1*H*-tetrazol-5-ol (two conformers, I and II).

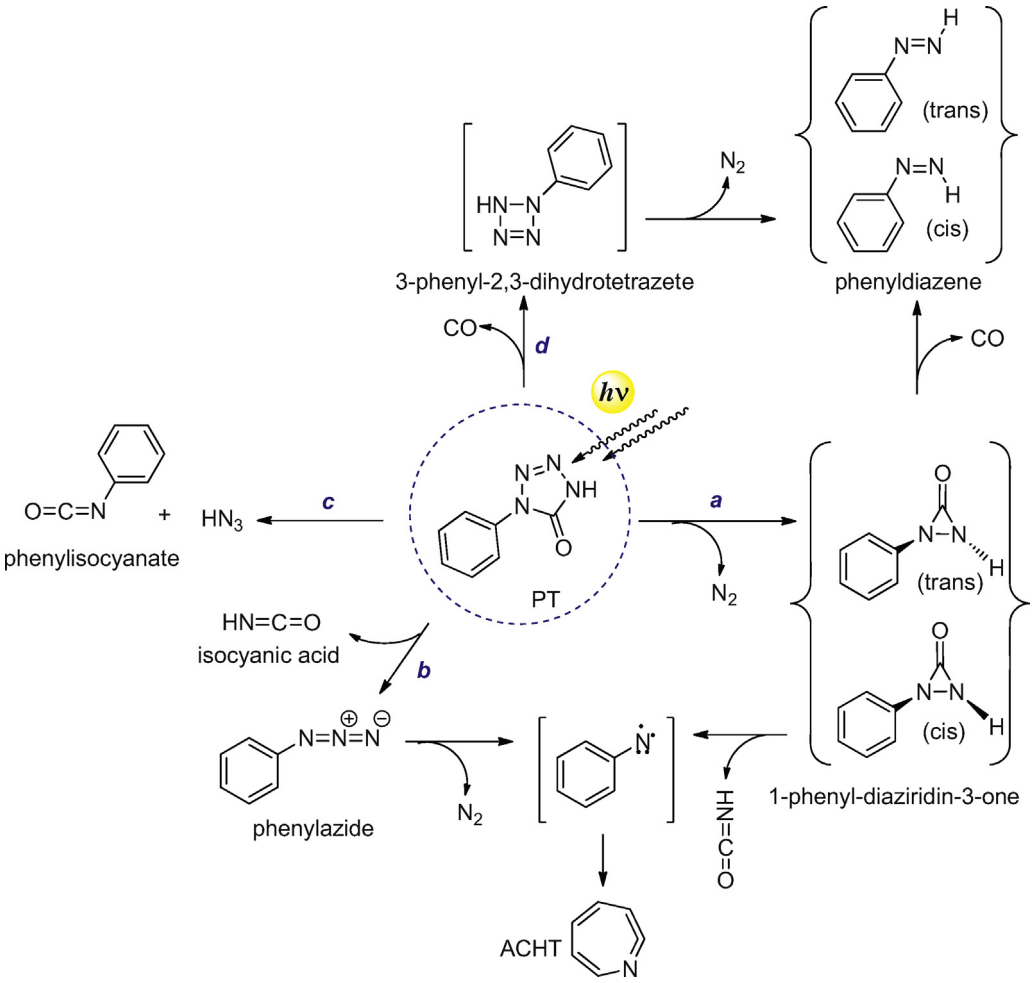

Scheme 6. Photochemical reactions observed for 1-phenyl-tetrazolone, isolated in solid argon, upon irradiation with UV (λ > 235 nm) light.

were observed at *ca.* 2263 (buried under the intense group of bands due to νNCO *as* of phenylisocyanate), 824 and 630 cm^{-1}, in fairly good agreement with the DFT(B3LYP)/6−31++G(d,p) calculated frequencies for this molecule (2287, 850 and 627 cm^{-1}, respectively) [22]. Since the bands assigned to phenylazide still continued to grow considerably after 60 min of irradiation, it was concluded that in this case phenylazide undergoes its usual subsequent reactions (as mentioned before, phenylazide tends to release N_2 and form phenylnitrene and then ACHT) only with relatively low efficiency.

Pathway ***c*** corresponds to tetrazole ring opening leading to phenylisocyanate and azide (see Scheme 6). No indications were found pointing to additional reactions of these compounds under the experimental conditions used [22]. The experimental spectrum of phenylisocyanate is readily identifiable because it shows a very characteristic intense multiplet in the 2290–2260 cm^{-1} region (Fig. 8) due to the νNCO antisymmetric stretching vibration that clearly dominates the spectrum of the photolyzed matrix. According to the theoretical predictions, the intensity of such unusually intense band represents about 90% of the total intensity of the spectrum of phenylisocyanate. The bands corresponding to azide could also be identified in the spectra of the irradiated matrix by comparison with the spectrum of the matrix-isolated azide previously reported by Himmel et al. [59].

A fourth possible reaction pathway (pathway ***d***; see Scheme 6) could not be discarded (though it could not be doubtlessly proved in our study [22]). This reaction channel can lead to production of phenyldiazene through initial elimination of CO (to yield phenyltetrazete) followed by N_2 extrusion.

It is interesting to notice here that for 5MPT, 5EPT and PT all the primary photochemical reactions imply simultaneous cleavage of two single bonds in the tetrazole ring of the reactant molecule. Compared to PT, the number of single bonds in both 5MPT and 5EPT tetrazole rings is reduced from 4 to 3, and the number of observed primary photochemical processes decreases from 3 (or 4, depending if pathway ***d*** in PT is effectively active or not) to 2. Indeed, as it will be shown in the next sections, this trend appears to be a general rule for tetrazole derivatives.

2.8. 1-Phenyl-4-allyl-tetrazolone (APT)

The relevance of allyltetrazole derivatives in organic synthesis attaches ever increasing interest to their study. Particularly, the title compound of this subsection is an important precursor of other biologically active heterocycles, through photolysis [60,61], and may be obtained from the corresponding 5-allyloxytetrazoles in quantitative yields through a thermally induced Claisen-type isomerization [62–66]. Furthermore, allyltetrazolones are important structural units of biologically active systems, acting as key intermediates in the biosynthesis of several important biomolecules [67–69].

As can be observed from Fig. 9, the structure of APT differs from that of 1-phenyl-tetrazolone (PT) in the replacement of the hydrogen linked to the tetrazole ring by an allyl group. Thus, one can expect that the observed differences in their photochemistry result essentially from this relevant structural modification. In addition is the increase in conformational freedom brought by the allylic

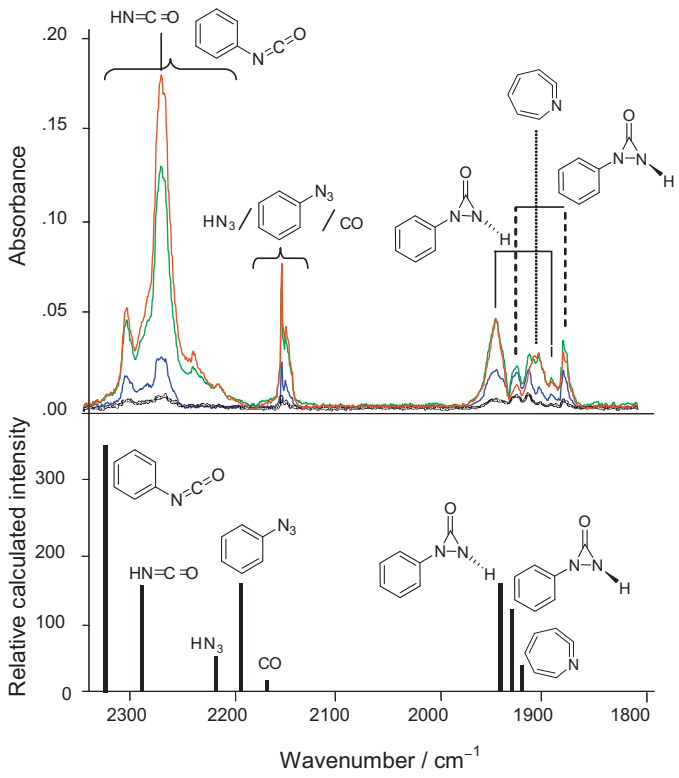

Fig. 8. 2350–1800 cm^{-1} spectral region of the irradiated ($\lambda > 235$ nm) matrix of 1-phenyl-tetrazolone at different times of irradiation [2 (black line), 10 (blue), 30 (green) and 60 (red) min] and B3LYP/6−311++G(d,p) calculated spectra, in this spectral range, for the observed photoproducts. (For interpretation of the references to color in this figure legend, the reader is referred to the web version of the article.)

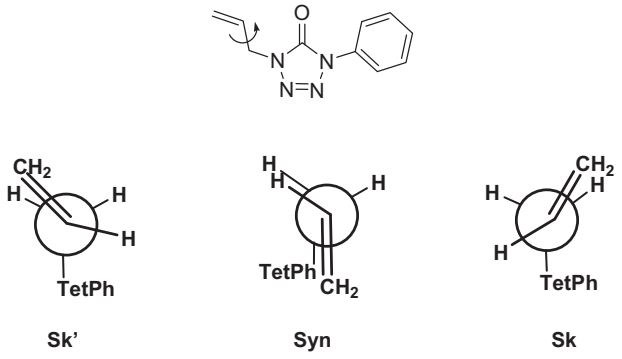

Fig. 9. Minimum energy conformations of 1-phenyl-4-allyl-1,4-dihydro-5*H*-tetrazol-5-one [24]: Sk′, Syn and Sk (represented as Newman projections). The lowest-energy structure was found to be conformer Sk′. Note that the tetrazole and phenyl rings are coplanar, but the CH=CH$_2$ fragment stays nearly perpendicular to the plane of the rings. This makes forms Sk and Sk′ to be non-equivalent by symmetry.

substituent might also be thought to open the possibility of other exit channels from photolysis.

All minimum energy conformations in APT differ on the orientation of the −CH=CH$_2$ group on the allylic chain relatively to the tetrazole ring. Three conformers were found on the potential energy surface of the molecule (Fig. 9). In these, the N−CH$_2$−CH=CH$_2$ dihedral angle is *ca.* −123° (Sk′), 121° (Sk) and −2° (Syn) [24] and their relative populations in the gas phase prior to deposition, as predicted by DFT(B3LYP)/6−311++G(d,p) calculations, are 41.8%, 38.8% and 19.4%, respectively [24].

Somewhat surprisingly, we found that the photochemistry exhibited by matrix-isolated APT is not significantly influenced by the conformation of the allyl group. Indeed, matching closely the general scheme for the photochemistry of phenyltetrazolic compounds, the following photolysis pathways were identified for matrix-isolated APT (Scheme 7): (**a**) N_2 elimination with formation of 1-allyl-2-phenyldiaziridin-3-one (APD) which partially reacts further to form 1-allyl-1*H*-benzoimidazol-2(3*H*)-one (ABZ); (**b**) ring cleavage to form allyl isocyanate and phenyl azide (and then ACHT) and (**c**) ring cleavage to form phenylisocyanate and allyl azide. Interestingly, the allylic chain is maintained intact in all observed photochemical processes, indicating the photochemical stability of this residue under the experimental conditions used and justifying the lack of relevance of the presence in the matrix of several conformers to the observed photochemistry.

After 40 min of irradiation, 48% of the reactant initially present in the matrix had been consumed (see Fig. 10). Considering the relative amounts of the photoproduced species extracted from the experimental spectra (calculated spectra were used as reference data for normalization of the intensities), it was possible to determine the relative efficiencies of the different reaction channels as being *b*:*c*:*a* = 8:16:24%.

Very interestingly, the observed photochemistry of the matrix-isolated APT is distinct from the preferred photochemical fragmentation in solution, where a different heterocycle, 3,4-dihydro-3-phenyl-pyrimidin-2(1*H*)-one, is produced as the major photoproduct [20,60]. The lack of formation of phenyl-pyrimidinone from photolysis of matrix-isolated APT is doubtlessly related with the matrix environment where the reaction is suppressed. We believe that a strong restriction of conformational mobility in the argon matrix affects not only APT itself, but also its photoproducts. The design of phenyl-pyrimidinone from APT (after extrusion of N_2) involves an approach between the terminal carbon of the allylic chain and the nitrogen atom N-1, in order to form a new C—N single bond. Such approach is most probably strongly hindered in the rigid matrix. On the other hand, formation of ABZ appears as the main photoreaction channel for APT, in keeping with the results reported by Quast and Nahr [70].

The photochemistry of matrix-isolated 1-phenyl-tetrazolone and APT differ mainly in the secondary fragmentation pathways, essentially because the labile (and much smaller, when compared with the allyl fragment) hydrogen atom in 1-phenyl-tetrazolone confers to the primary photoproducts produced from this compound more flexibility regarding possible subsequent photochemical reactions, in particular under volume-restricted conditions as it is the case of a solid matrix.

2.9. 1-Allyltetrazole (1-ALT) and 2-allyltetrazole (2-ALT)

In 1-ALT and 2-ALT, the orientation of the allyl moiety with regard to the tetrazole ring gives rise to different conformers, whose relative energies stay within 3.5 kJ mol^{-1} [71]. UV irradiation ($\lambda > 280$ nm) of the compounds in argon matrices led to relatively slow consumption of all three conformers of each molecule. Very interestingly, irradiation of both precursors led to the same photoproducts, suggesting a common intermediate, 1-allyl-1*H*-diazirine (Scheme 8).

The main photolysis pathway proceeded through the tetrazole ring cleavage, N_2 elimination and formation of N-allylcarbodiimide as the main product. Two other species, allylcyanamide and allylnitrilimine were also detected in the irradiated matrices (Scheme 8).

2.10. Tetrazole coupled with another heterocycle

Heterocycles find wide applications in coordination chemistry as ligands and, among them tetrazoles are known to play an

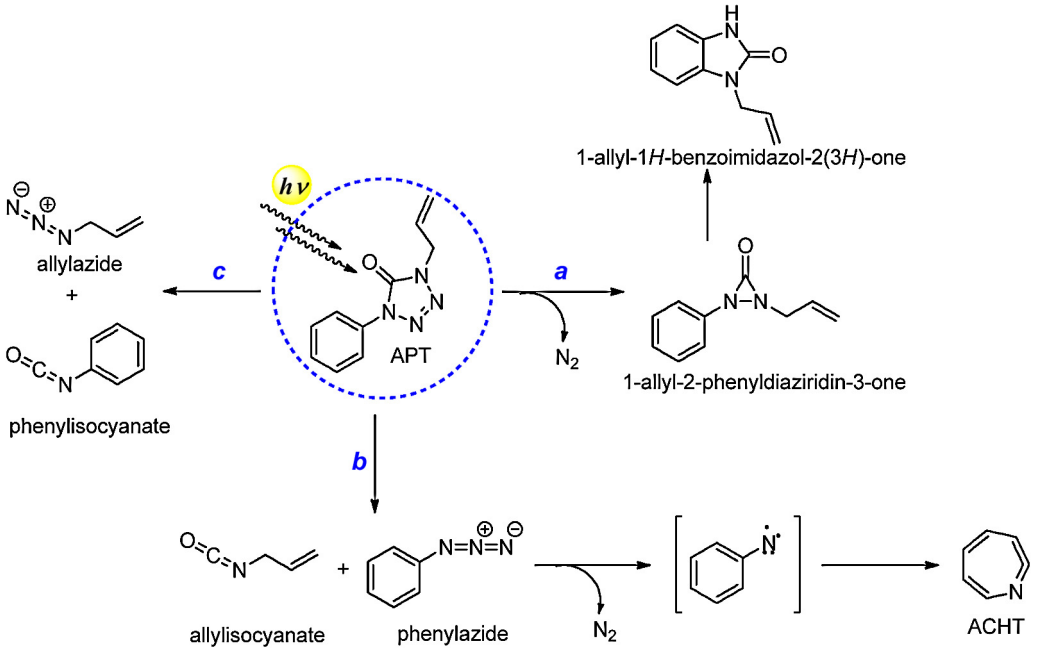

Scheme 7. Photochemical reactions observed for 1-phenyl-4-allyl-1,4-dihydro-5*H*-tetrazol-5-one isolated in an argon matrix upon irradiation with UV (λ > 235 nm) light.

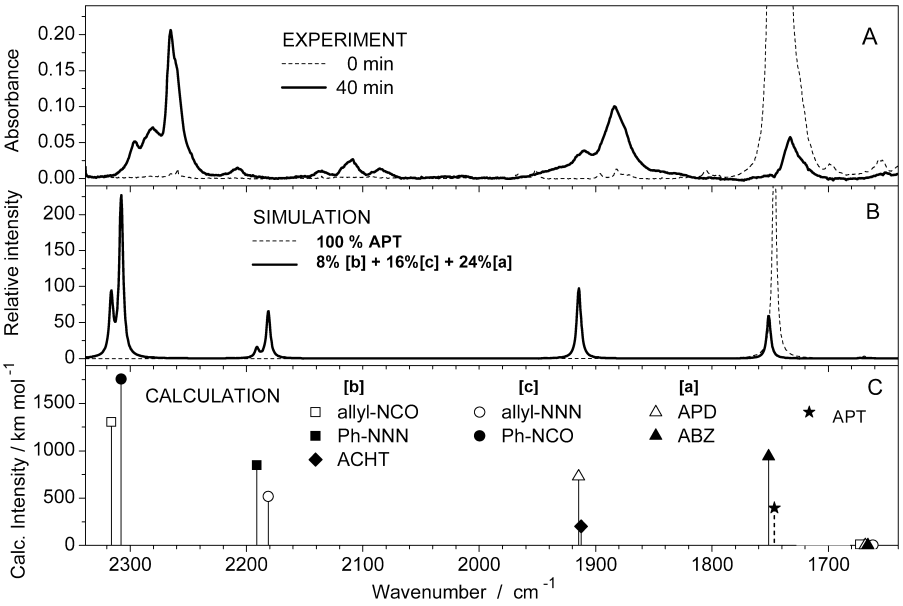

Fig. 10. Infrared spectra of APT and the proposed photoproducts, in the carbonyl stretching region. (A) dashed line – FTIR spectrum of the as-deposited matrix of APT (argon, 10 K); solid line – extracted spectrum of the photoproducts formed after 40 min of UV-irradiation (λ > 235 nm). (B) Simulated infrared spectra of APT (dashed line) and a mixture of photoproducts (solid line). The calculated intensities in the spectrum of APT were taken as 100%. The calculated intensities of photoproducts were scaled down to reproduce the relative intensities in the experimental spectrum of photoproducts and to obey the normalization condition: total amount of photoproducts is equal to the amount of consumed reagent (48%). (C) DFT(B3LYP)/6−311++G(d,p) calculated spectra of APT (dashed sticks) and possible photoproducts. The calculated wavenumbers were scaled with a uniform factor of 0.978. The calculated intensities were not scaled. Groups [a], [b] and [c] designate different photochannels.

important role. It has been demonstrated that the heterocycle tetrazole is able to participate in at least nine distinct types of coordination modes with metal ions in the construction of novel metal-organic frameworks [72]. In addition to the relevance of tetrazoles as ligands in catalysis, the coordination ability of the tetrazolyl ligand through four nitrogen electron-donating atoms allows it to serve as a bridging building block in supramolecular assemblies [72]. Especially relevant in this context are bis-tetrazole molecules or conjugates where the tetrazole ring is linked to other heterocycles. In all these systems, a detailed investigation of the structure, including tautomeric and conformational preferences of the molecules, and of their thermal and photochemical stability, is of crucial relevance to define properties and function.

Recently, tetrazole-triazole, tetrazolylpyridines and tetrazole-benzisothiazole conjugates were studied, with the aim of exploring their potential as multidentate nitrogen ligands.

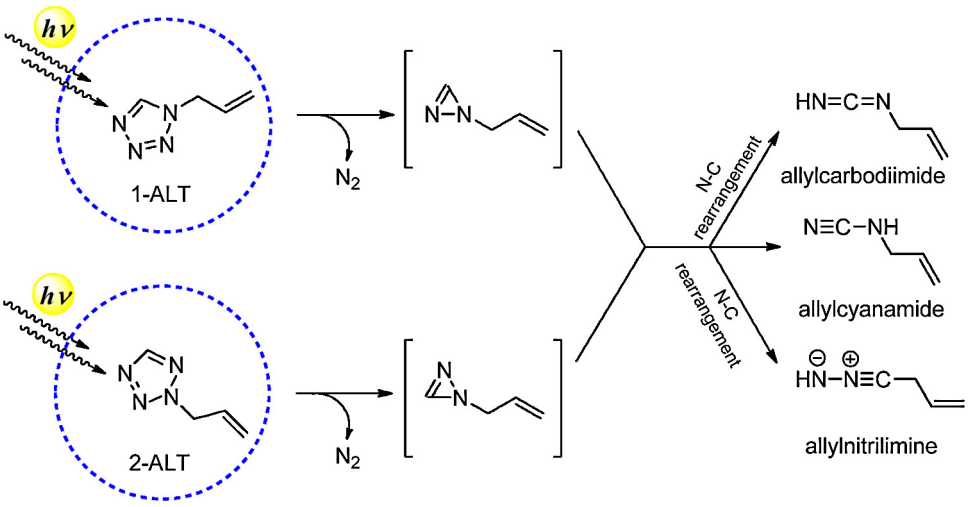

Scheme 8. Photochemical reactions observed for 1-allyltetrazol (1-ALT) and 2-allyltetrazol (2-ALT), isolated in solid argon, upon irradiation with UV (λ > 280 nm) light.

In all classes tetrazole is connected to another electron-withdrawing heterocycle, directly or through a linker. Some of the molecules prepared were deeply investigated regarding their structure and/or their photochemical stability, as is the case for 5-(1*H*-tetrazol-1-yl)-1,2,4-triazole, 2-(tetrazol-1-yl)-, 3-(tetrazol-1-yl)- and 2-(tetrazol-5-yl)pyridines and 2-[1-(1*H*-tetrazol-5-yl)ethyl]-1,2-benzisothiazol-3(2*H*)-one 1,1-dioxide [27,41,73–76]. The matrix photochemistry of these conjugates, described below, led to the identification and characterization of new molecules: 1*H*-1,2,4-triazol-5-yl carbodiimide, 1*H*-1,2,4-triazol-3-yl carbodiimide, pyridin-2-yl carbodiimide, pyridin-3-yl carbodiimide, 1-cyclopenta-2,4-dienylketenimine, 2-[1-(1*H*-diaziren-3-yl)ethyl]-1,2-benzisothiazol-3(2*H*)-one 1,1-dioxide, 2-(1,1-dioxide-3-oxo-1,2-benzisothiazol-2(3*H*)-yl)propanenitrile and 7-thia-8-azabicyclo[4.2.0] octa-1,3,5-triene 7,7-dioxide.

2.10.1. 5-(1H-tetrazol-1-yl)-1,2,4-triazole (T)

In the studied tetrazole-triazole conjugate both heterocycles are directly connected through a C-N bond (Fig. 11). The 5-(1*H*-tetrazol-1-yl)-1,2,4-triazole molecule (T) may exist in five tautomeric forms, differing by the position of the H atom in the triazole ring. The tautomers of T will be named here according to the triazole ring atom number where the annular hydrogen atom is attached, from T1 to T5 (Fig. 11). According to calculations (B3LYP/6−311++G(2d,2p)) [41], the lower energy minima correspond to tautomers T1, T2 and T4, where the annular H atom is attached to nitrogen atoms N-1, N-2 and N-4 of the triazole ring. In the global minimum (T1), the annular H-7 atom is attached to the N-1 atom of triazole and this structure is stabilized by a favorable NH···N inter-ring interaction. The next in stability order are two conformers of the T2 tautomer: T2a and T2b (relative energies: 3.6 and 6.9 kJ mol^{-1}, respectively), followed by tautomer T4 (24.6 kJ mol^{-1}). In T4, despite the existence of the same NH···N inter-ring stabilizing interaction as in T1, the relative energy is much higher. This observation was ascribed to the destabilizing effect introduced by two vicinal nitrogen atoms in triazole ring (N-1 and N-2) having the same hybridization. Similar destabilizing effect of such neighborhood was encountered in other molecules [77].

The calculations revealed also the existence of two pairs of conformers of high energy isomers of the compound (T3a, T3b) and (T5a, T5b), in which the annular hydrogen is connected to the C-3 or C-5 atoms, respectively [41].

Bands due to both tautomers T1 and T2 can be identified in the experimental spectrum of a freshly deposited sample. Moreover, trapping T in xenon matrices at 15 K, and subsequent heating of the sample to temperatures to ∼30 K (annealing) permitted to induce conformational transformation between conformers T2a and T2b (see Fig. 12), while the population of T1 was not affected by such procedure. This experiment enabled unequivocal spectroscopic characterization of each form and to establish the experimental

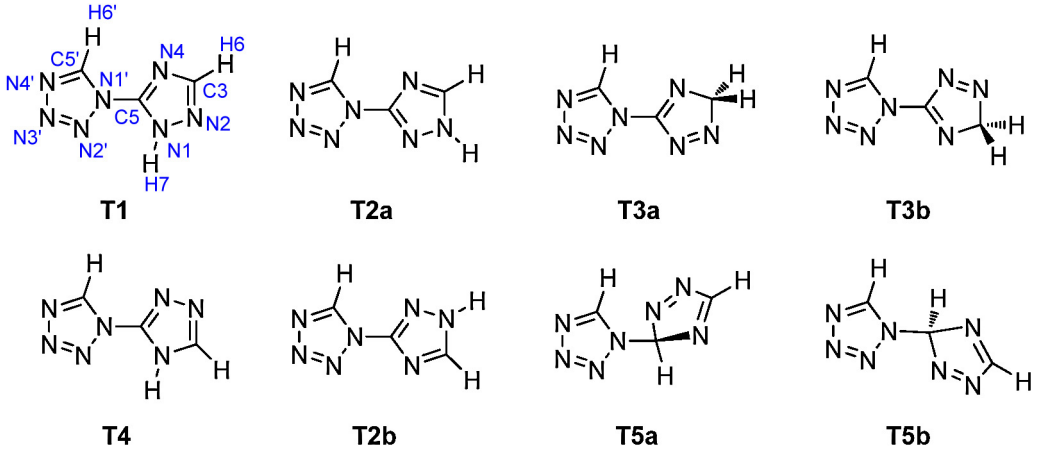

Fig. 11. Tautomers (T1-T5) and conformers (a/b) of tetrazolyl-triazole.

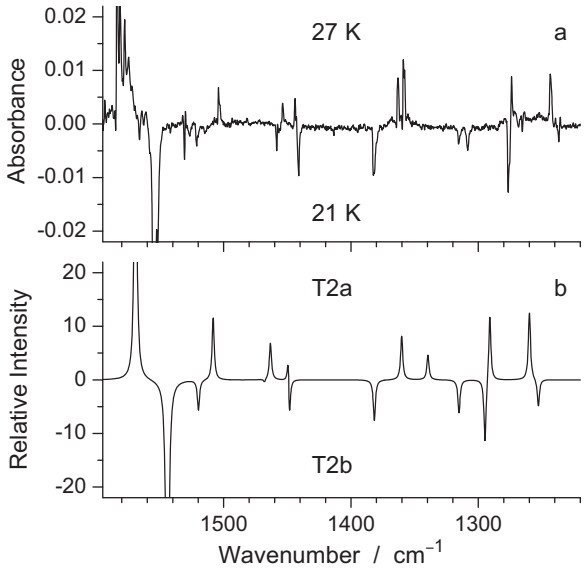

Fig. 12. IR spectra of T: (a) experimental difference spectrum of T isolated in a xenon matrix, showing changes upon annealing occurring in the temperature interval from 21 K to 27 K. The growing bands show upwards; (b) simulated difference spectrum between the theoretically calculated spectra of T2a (positive bands) and T2b (negative bands) constructed as "T2a" minus "T2b". The theoretical spectra were simulated with Lorentzian functions (fwhm = 2 cm^{-1}) centered at the B3LYP/6−311++G(2d,2p) calculated frequencies (scaled by 0.984).

conditions to use during the photochemical studies, where the conformational composition of the molecule was reduced to only two structures (T1 and T2a).

The most spectacular behavior of matrix isolated tetrazolyltriazole is its tautomer-selective photochemistry (a similar feature was observed, and discussed above, for 1-(tetrazol-5-yl)ethanol (TE) isolated in solid argon [26]). UV irradiation (λ > 288 nm) of the compound in xenon matrix led to fast consumption of tautomer T1 (*ca.* 50% in 5 min, almost complete depletion after 30 min), while T2a remained intact. Simultaneously, new bands appeared in the spectrum of the irradiated sample, which must be due to a photochemical product (P1). Upon subsequent irradiation of the matrix with UV-light of shorter wavelengths (λ > 234 nm), the bands due to the T2a tautomer strongly decreased during 25 min of photolysis. At the same time, a set of bands showed up in the spectra, which are due to a second photoproduct (P2).

Fig. 13 shows representative changes in the experimental T/Xe spectra occurring in the process of photolysis with λ > 288 nm filter for T1 and with λ > 234 nm filter for T2a. These changes compared with theoretical simulations showing selective transformations of the T1 and T2a tautomers into the suggested photoproducts, P1 and P2, whose structure is discussed below. Similar broad band UV irradiations (λ > 288 nm and λ > 234 nm) applied to T isolated in argon matrices led to the appearance of sets of bands corresponding to the same photoproducts as observed in xenon matrices.

The main photochemistry pathways resulting from irradiation of the T1 and T2a species in the studied matrices are schematically shown in Scheme 9. The N_2 elimination pathway and formation of carbodiimide is the dominating route of the T photolysis. Both T1 and T2a tautomers photolyze according to the same pathway, yielding analogous products differing in the position of the H-atom attached to the triazole ring, 1*H*-1,2,4-triazol-5-yl carbodiimide (P1) and 1*H*-1,2,4-triazol-3-yl carbodiimide (P2). The set of bands appearing first in the spectra, at the expense of T1, when lower energy radiation (λ > 288 nm) was applied, fits nicely the calculated spectrum of carbodiimide P1. In turn, the group of bands appearing at the expense of T2, when higher energy radiation (λ > 234 nm) was applied fits very well the carbodiimide P2 spectrum.

According to calculations, the N—N bonds that undergo cleavage in the observed photoreactions are the tetrazole weakest, formally single bonds, longer than 1.360 Å. The formation of the P1 and P2 products proceeds most probably through the 1-(1*H*-1,2,4-triazol-5-yl)diaziridine and 1-(1*H*-1,2,4-triazol-3-yl)diaziridine intermediates (Scheme 9). However, these species seem to be rather unstable and were not detected experimentally.

The observed preference for the reaction path leading to the carbodiimide plus N_2 is in agreement with the calculated ground-state reaction energies, which are also provided in Scheme 9. It is known that 1,5-disubstituted tetrazoles are useful precursors of carbodiimides (R—N=C=N—R'), while 1-substituted tetrazoles give rise to monosubstituted carbodiimides R—N=C=N—H. The latter molecules were found to be stable at low temperatures, but isomerize to cyanamides RNH—CN at ordinary temperatures [78].

2.10.2. 2-(Tetrazol-1-yl)pyridine (Py2T), 3-(tetrazol-1-yl) pyridine (Py3T) and 2-(tetrazol-5-yl)pyridine (PyT)

The title compounds of this subsection are tetrazole derivatives where the tetrazole ring is coupled with the *ortho* carbon of a

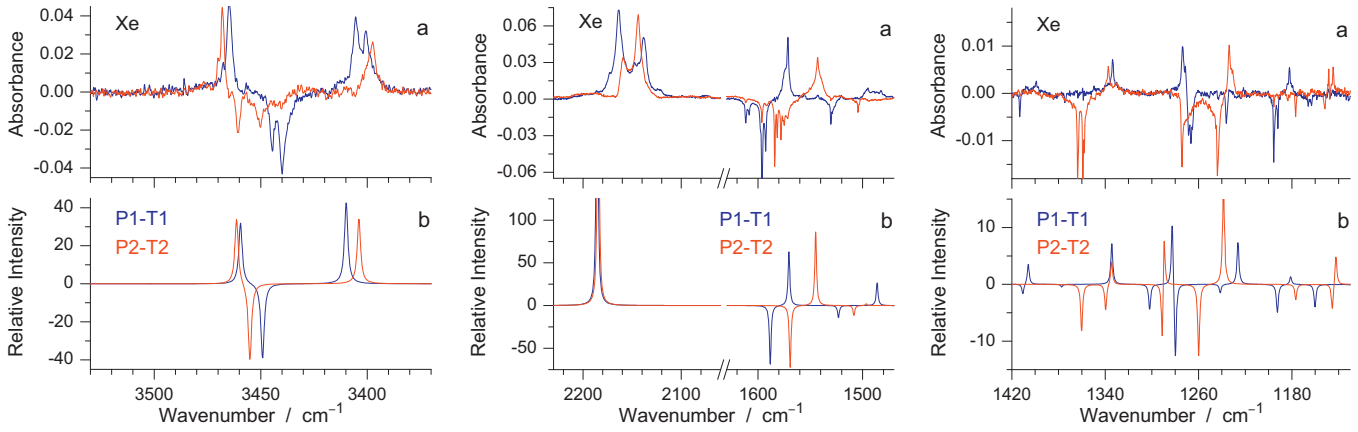

Fig. 13. (a) Experimental difference spectra of T isolated in a xenon matrix at 30 K. Blue trace: changes after 15 min of UV irradiation with light λ > 288 nm. Red trace: changes after 25 min of additional UV irradiation with light λ > 234 nm (subsequent to irradiation with λ > 288 nm). Growing bands show upwards; (b) simulated difference spectra constructed as "P1 minus T1" (blue trace) and "P2 minus T2a" (red trace). The theoretical spectra were simulated with Lorentzian functions (fwhm = 2 cm^{-1}) centered at the B3LYP/6−311++G(2d,2p) calculated frequencies and scaled by 0.945 (above 3000 cm^{-1}) and 0.984 (below 3000 cm^{-1}). Positive bands are due to P1 (blue) and P2 (red), negative bands are due to T1 (blue) and T2a (red). (For interpretation of the references to color in this figure legend, the reader is referred to the web version of the article.)

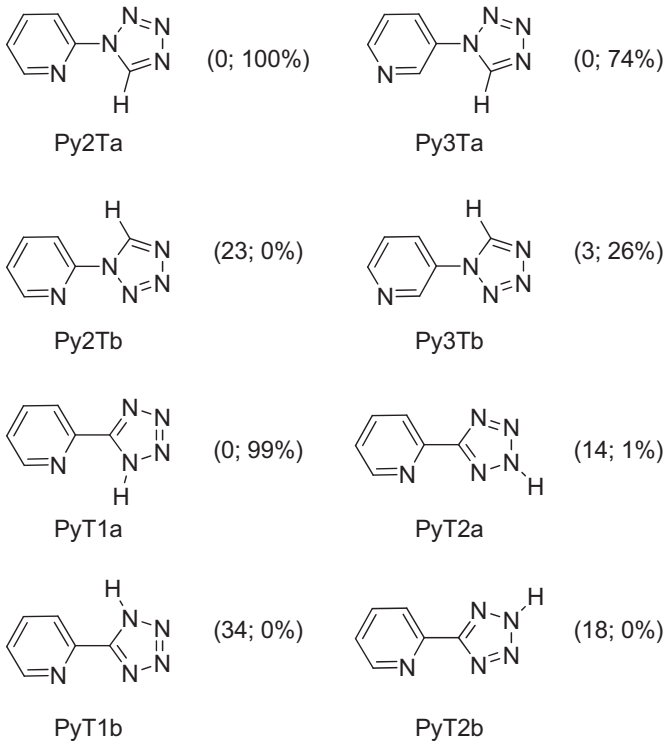

Fig. 14. Py2T, Py3T and PyT isomeric forms. Relative energies (kJ mol^{-1}) and expected population in gas phase at room temperature for the isomers of same compound in parentheses.

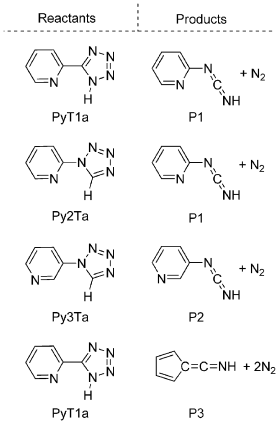

Fig. 15. Reactants and final products for the stepwise dissociations on the S_0 surface of PyT1a, Py2Ta and Py3Ta and subsequent P1, P2 or P3 formation. For the detailed mechanisms of these reactions see Ref. [73].

pyridine ring through the N-1 [2-tetrazol-1-yl pyridine (Py2T), 3-tetrazol-1-yl pyridine (Py3T)] or through C-5 atom [2-tetrazol-5-yl pyridine (PyT)].

Py2T and Py3T have one internal rotation axis that gives rise to two different conformational isomers denoted as Py2Ta, Py2Tb and Py3Ta, Py3Tb, respectively [73].

PyT may exist in two tautomeric forms differing in the position of the hydrogen atom in the tetrazole ring. For both PyT tautomers two conformers may exist with different arrangement of the two rings in the molecule, giving altogether four stable forms. All these structures are presented in Fig. 14, where relative energies of the different forms for each compound and their expected gas-phase population at room temperature are also provided. According to the predicted relative energies, in the as deposited argon matrices of the compounds only Py2Ta and PyT1a can be isolated, while in the case of Py3T two conformers could be trapped: Py3Ta and Py3Tb.

Broad-band irradiation of the Py2Ta, Py3Ta/Py3Tb ($\lambda \leq 280$ nm) and PyT1a ($\lambda \leq 305$ nm) species led to cleavage of the tetrazole ring, with the elimination of N_2 and the simultaneous formation of pyridin-2-ylcarbodiimide (P1) or pyridin-3-ylcarbodiimide (P2) (Fig. 15). In spite of the different structure of the Py2Ta and PyT1a precursors, the same photoproduct P1 was detected for both species indicating that a carbon-to-nitrogen rearrangement took place in the case of the PyT1a molecule. An additional, unique for the PyT1a precursor, reaction pathway was found consisting in two N_2 molecules elimination and leading to 1-cyclopenta-2,4-dienylketenimine (P3) as a final photoproduct (Fig. 15).

2.10.3. 2-[1-(1H-tetrazol-5-yl)ethyl]-1, 2-benzisothiazol-3(2H)-one 1,1-dioxide (1-TE-BZT)

The design of tetrazole-saccharinates was envisaged recently, based on the known versatility of tetrazoles [72], saccharin (1,

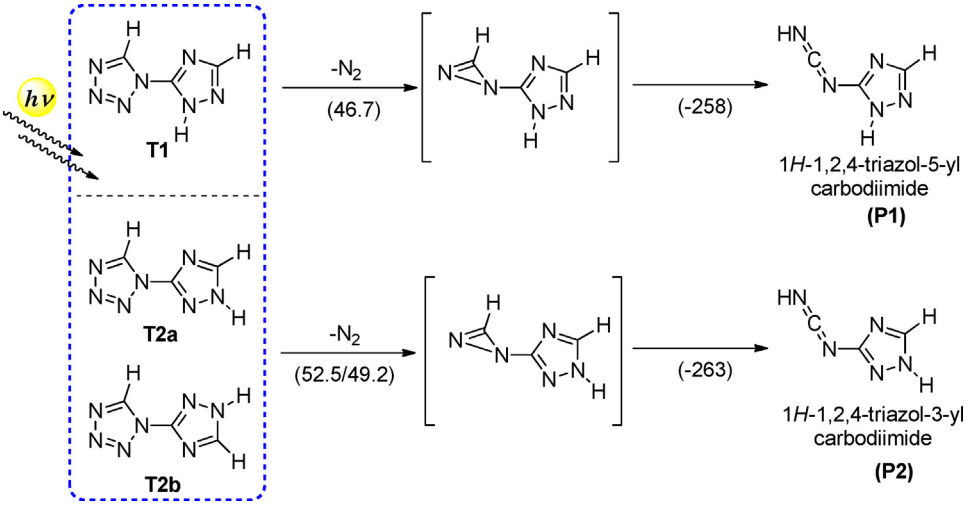

Scheme 9. The main photochemistry pathways resulting from irradiation of the T/Ar and T/Xe matrices. The calculated ground-state reaction energies (ZPE corrected, kJ mol^{-1}) are also shown.

1*H* Tautomer

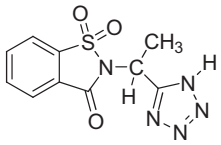

2-[1-(1*H*-tetrazol-5-yl)ethyl]-1,2-benzisothiazol-3(2H)-one 1,1-dioxide

2*H* Tautomer

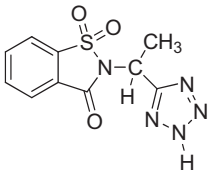

2-[1-(2*H*-tetrazol-5-yl)ethyl]-1,2-benzisothiazol-3(2H)-one 1,1-dioxide

Fig. 16. 1*H* and 2*H* tautomers of the tetrazole-saccharinate 1-TE-BZT.

2-benzisothiazol-3(2*H*)-one 1,1-dioxide) and saccharinate [79] as coordinating ligands [37]. One of these was 2-[1-(1*H*-tetrazol-5-yl)ethyl]-1,2-benzisothiazol-3(2*H*)-one 1,1-dioxide (1-TE-BZT), a tetrazole-saccharyl conjugate where the heterocycles are connected by an alkyl group. The structure and matrix photochemistry of 1-TE-BZT were investigated using vibrational spectroscopy and quantum chemical calculations [DFT(B3LYP)/6−311++G(3df,3pd)] [27].

1-TE-BZT has a chiral centre, the two enantiomers (R and S forms) being spectroscopically equivalent. The compound may exist in two tautomeric forms (Fig. 16), both having two conformationally relevant internal degrees of rotation, which are defined by the bridging N—C and C—C bonds.

Calculations predicted a total of 6 minima on the ground state potential energy surface of 1-TE-BZT: four minima correspond to the conformers of tautomer 1*H* and the remaining two to the conformers of tautomer 2*H*. According to calculations, conformers belonging to the 1*H* tautomer were found to be the most stable forms. The stabilization of these forms results from the presence of an intramolecular hydrogen bond-like interaction (NH···O=X, where X = S, C) that is absent in both the 2*H* conformers.

Irradiation of 1-TE-BZT (λ = 275 nm) deposited in a solid argon matrix (only the most stable structure of 1*H* tautomer was observed in the matrix) induced a prompt decrease of the 1-TE-BZT bands in their IR spectrum with a concomitant observation of new bands corresponding to the photoproduced species. The interpretation of these new bands led to a proposal of different pathways for the photodecomposition of 1-TE-BZT in solid argon Scheme 10 [27], comprising: (a) photocleavage of the tetrazole ring with extrusion of N_2 leading to formation of 2-[1-(1*H*-diaziren-3-yl)ethyl]-1,2-benzisothiazol-3(2*H*)-one 1,1-dioxide; (b) photocleavage of the tetrazole ring leading to formation of azide (N_3H) and 2-(1,1-dioxide-3-oxo-1,2-benzisothiazol-2(3*H*)-yl)propanenitrile; (c) photocleavage of the saccharyl ring (decarbonylation) and of the tetrazole ring, with formation of azide (N_3H), 7-thia-8-azabicyclo[4.2.0] octa-1,3,5-triene 7,7 dioxide and propene-nitrile.

The relative intensity of bands in the experimental IR spectra of the photolysed matrices indicate that the amount of photoproducts generated in pathway ***c*** is higher than that of the photoproducts from pathways ***a*** and ***b***. Thus, it appears that the pathway involving photocleavage of both the saccharyl and the tetrazolyl rings, is the preferred photodecomposition channel for 1-TE-BZT [27]. Although the photodecomposition of saccharin's in solution was known [80,81], these results were surprising, since they brought the first observation of photoinduced cleavage of the saccharyl core in matrix photochemistry of saccharyl derivatives, leading to decarbonylation. The UV-induced photoisomerization of saccharin in solid argon has been reported very recently, leading to a new compound, isosaccharin [82]. Photolysis of 1-TE-BZT isolated in solid argon led to formation and characterization of three new molecules, specifically: 2-[1-(1*H*-diaziren-3-yl)ethyl]-1,2-benzisothiazol-3(2*H*)-one 1,1-dioxide, 2-(1,1-dioxide-3-oxo-1,2-benzisothiazol-2(3*H*)-yl)propanenitrile and 7-thia-8-azabicyclo[4.2.0] octa-1,3,5-triene 7,7 dioxide.

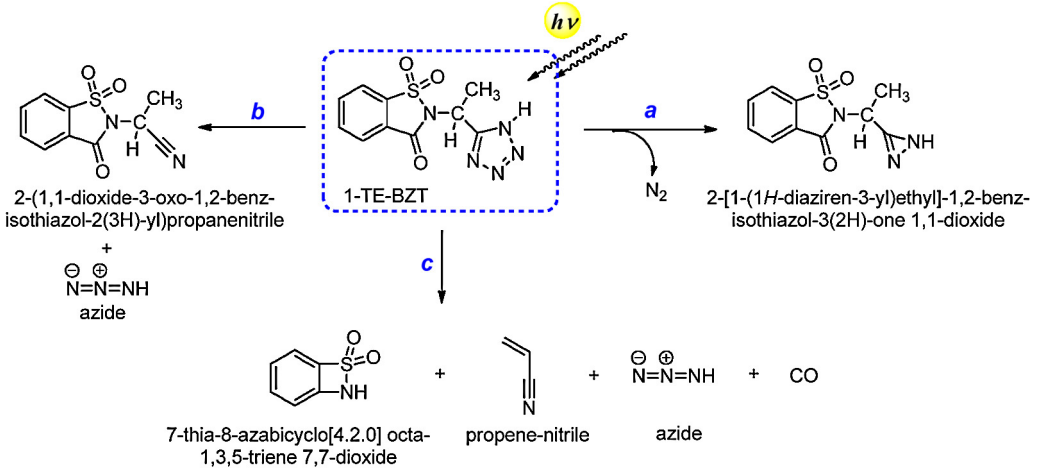

Scheme 10. Photochemical reactions observed for 2-[1-(1*H*-tetrazol-5-yl)ethyl]-1,2-benzisothiazol-3(2*H*)-one 1,1-dioxide isolated in an argon matrix upon irradiation with UV (λ > 275 nm) light.

Table 1
Summary of the primary molecular species formed by photolysis of different matrix-isolated tetrazole derivatives.

Tetrazole derivative	*Primary photoproduced species*
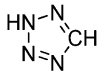	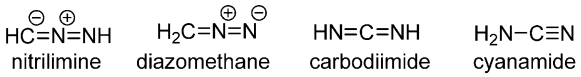 nitrilimine; diazomethane; carbodiimide; cyanamide
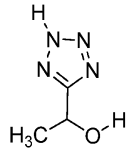	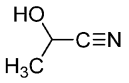 2-hydroxypropanenitrile
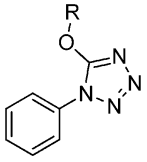 R = Me, Et	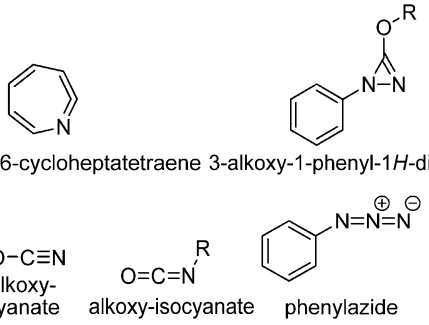 1-aza-1,2,4,6-cycloheptatetraene; 3-alkoxy-1-phenyl-1*H*-diazirine; alkoxy-cyanate; alkoxy-isocyanate; phenylazide
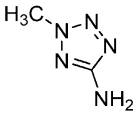	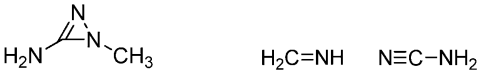 1-methyl-1*H*-diazirene-3-amine; methylenimine; cyanamide
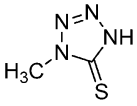	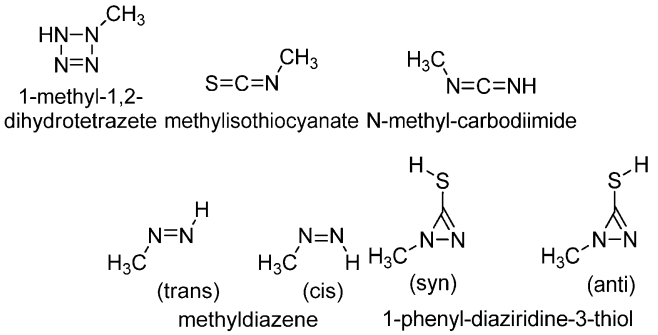 1-methyl-1,2-dihydrotetrazete; methylisothiocyanate; N-methyl-carbodiimide; methyldiazene (trans); methyldiazene (cis); 1-phenyl-diaziridine-3-thiol (syn); 1-phenyl-diaziridine-3-thiol (anti)
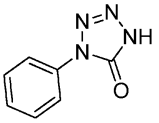	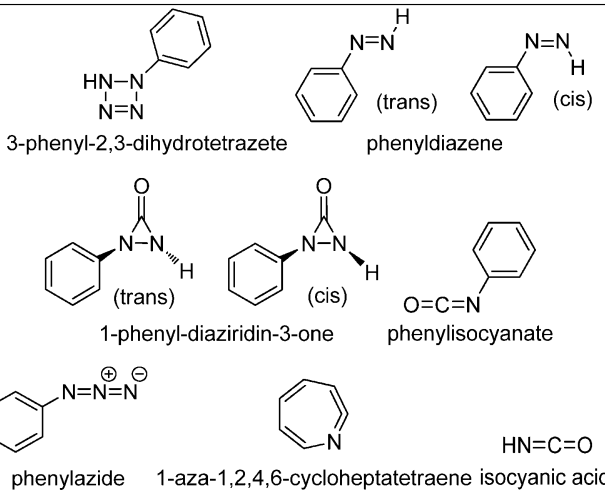 3-phenyl-2,3-dihydrotetrazete; phenyldiazene (trans); phenyldiazene (cis); 1-phenyl-diaziridin-3-one (trans); 1-phenyl-diaziridin-3-one (cis); phenylisocyanate; phenylazide; 1-aza-1,2,4,6-cycloheptatetraene; isocyanic acid

Table 1 (*Continued*).

Table 1.*(continued)*

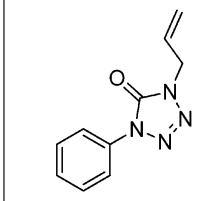

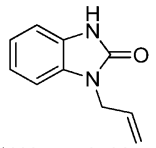

1-allyl-1*H*-benzoimidazol-2(3*H*)-one

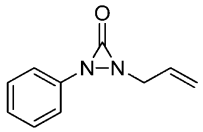

1-allyl-2-phenyldiaziridin-3-one

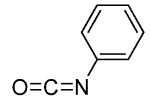

phenylisocyanate

1-aza-1,2,4,6-cycloheptatetraene

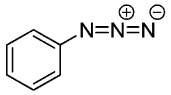

phenylazide

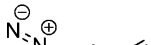

allylazide

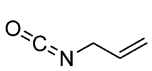

allylisocyanate

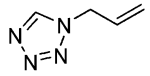

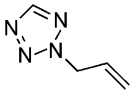

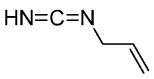

allylcarbodiimide

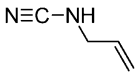

allylcyanamide

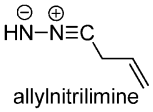

allylnitrilimine

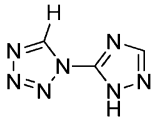

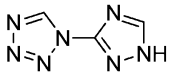

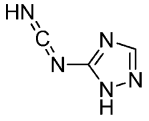

1*H*-1,2,4-triazol-5-yl carbodiimide

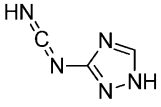

1*H*-1,2,4-triazol-3-yl carbodiimide

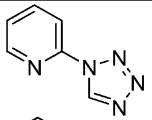

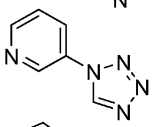

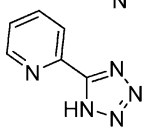

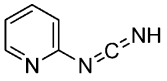

pyridin-2-yl carbodiimide

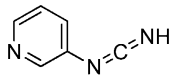

pyridin-3-yl carbodiimide

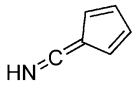

1-cyclopenta-2,4-dienylketenimine

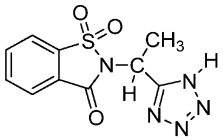

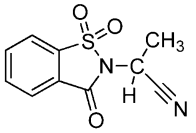

2-(1,1-dioxide-3-oxo-1,2-benz-isothiazol-2(3H)-yl)propanenitrile

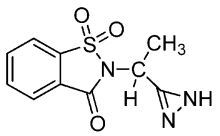

2-[1-(1*H*-diaziren-3-yl)ethyl]-1,2-benz-isothiazol-3(2H)-one 1,1-dioxide

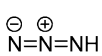

azide

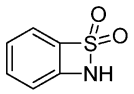

7-thia-8-azabicyclo[4.2.0] octa-1,3,5-triene 7,7-dioxide

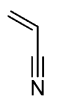

propene-nitrile

3. Conclusions

The use of matrix isolation technique coupled to a suitable probing method, such as FTIR spectroscopy, represents an accurate strategy to understand the mechanisms involved in photochemical reactions, its main advantages being the simplification of the photochemical processes due to cage confinement of the reactions and the possibility to achieve a high spectroscopic resolution, increasing the probability to detect chemical species produced in low amounts during photolysis or those with intrinsically low intensity IR absorptions. Then, matrix isolation represents then a powerful tool to investigate the photochemistry of tetrazole derivatives.

According to our results, the fundamental photochemistry of matrix-isolated tetrazoles involves fragmentation of the tetrazole ring. The specific substituents present in the ring determine in large amount the preferences for the different available primary photochemical reaction channels and strongly determine secondary processes in which the initial photoproducts participate. As a general rule, the tetrazole ring can undergo photolytic cleavage in three different ways: (a) through the (N-1)—(N-2) and (N-3)—(N-4) bonds, releasing molecular nitrogen and forming a diazirine derivative; (b) through the (N-1)—(C-5) and (N-3)—(N-4) bonds and (c) through (N-1)—(N-2) and (N-4)—(C-5) bonds. In the two latter cases, the precise nature of the photoproducts varies depending on the substituents present in the tetrazole ring, but one of the products is always an azide, which then can undergo subsequent reactions, most of times eliminating N_2 to form the nitrene that then can further react to form the final product (*e.g.*, ACHT, produced by ring expansion of phenyl nitrene).

The number of available reaction channels correlates with the number of formally single bonds in the tetrazole ring. When four single bonds are present (like in tetrazolones or tetrazole-thiones), the 3 photochemical fundamental types of reactions can take place, a fourth reaction path being sometimes also activated, corresponding to cleavage through the (N-1)—(C-5) and (N-4)—(C-5) bonds. For all molecules we investigated exhibiting only three formally single bonds in the tetrazole ring, only two reaction channels were found to be active, with that corresponding to direct N_2 elimination always playing the most important role.

The presence in the ring or in the substituents of labile hydrogen atoms always increases the complexity of the photochemistry, mainly due to the occurrence of different tautomeric forms, whereas the conformational flexibility of the substituent may have effects difficult to predict *a priori*. These are strongly determined by the number and relative energies of the possible conformers and conformational interconversion barriers.

The presence of a phenyl substituent at N-1 (or N-4) in alkyloxy tetrazoles results in strong activation of the channel leading to production of phenylazide and the corresponding alkyl-cyanate (that undergoes major isomerization to the isocyanate). In tetrazolones and tetrazole-thiones, a phenyl or alkyl substituent at N-1 (or N-4) favors the pathway leading to direct production of the corresponding isocyanate or thioisocyanate, which is in general inhibited in the alkyloxy and allyloxy tetrazoles.

The mechanism for direct elimination of molecular nitrogen from the tetrazole ring was not yet fully explained, but it seems that it occurs mainly through the biradical intermediate [20,21] that subsequently undergoes cyclization and forms diazirine. The biradical has been recently observed in an investigation carried out in our laboratory on substituted tetrazoles in solution, by laser flash-photolysis [21]. The mechanisms for the remaining two prototype primary ring-cleavage photochemical reactions of the tetrazole ring are still to be investigated.

It is fortunate that most of the prevalent photoproducts of the photochemistry of tetrazole derivatives can be reliably identified by IR spectroscopy. In fact, three groups of bands, occurring in usually clean spectral regions allow easy identification of the main products resulting from the three fundamental paths in tetrazoles' photochemistry: diazirines and diaziridinones give rise to characteristic bands in the 1800–1900 cm^{-1} spectral region, azides have their most intense band around 2100 cm^{-1} ($\nu N{=}N^{+}{=}N^{-}$ antisymmetric stretching) and isocyanates strongly absorb in the 2290–2300 cm^{-1} range ($\nu N{=}C{=}O$ antisymmetric stretching).

A final note shall be made regarding the possibility of using the *in situ* photolysis of matrix-isolated tetrazoles to produce novel molecular species (see structures in Table 1), like for example antiaromatic diazirines, diaziridines, carbodiimides, nitriles, reactive isocyanates, azides and tetrazetes (*e.g.*, 3-methoxy-1-phenyl-1*H*-diazirine, 3-ethoxy-1-phenyl-1*H*-diazirine, 3-allyloxy-1-phenyl-1*H*-diazirine, 1-phenyl-diaziridin-3-one, 1-allyl-2-phenyldiaziridin-3-one, 1*H*-1,2,4-triazol-5-yl carbodiimide, 1*H*-1,2,4-triazol-3-yl carbodiimide, 1-methyl-1,2-dihydrotetrazete, 3-phenyl-2,3-dihydrotetrazete, allylisocyanate, allylazide).

Acknowledgements

The authors are grateful to Fundação para a Ciência e Tecnologia (FCT, Portugal), FEDER and COMPETE-QREN-EU [Projects PEst-C/MAR/LA0015/2011, PTDC/QUI-QUI/111879/2009; PTDC/QUI-QUI/118078/2010, FCOMP-01-0124-FEDER-021082, and Grant SFRH/BPD/43853/2008 (L.M.T.F.)]. A.G.Z. [member of the research Career from the Argentinean National Research Council (CONICET)] acknowledges support from the Argentinean Agency for the Scientific and Technical Promotion [(ANPCyT) Project PICT(2011)/0226].

References

[1] R.J. Herr, Bioorganic & Medicinal Chemistry 10 (2002) 3379.
[2] G. Sandmann, C. Schneider, P. Boger, Zeitschrift für Naturforschung C, A Journal of Biosciences 51 (1996) 534.
[3] C. Zhao-Xu, X. Heming, International Journal of Quantum Chemistry 79 (2000) 350.
[4] G.I. Koldobskii, V.A. Ostrovskii, V.S. Poplavskii, Khimiya Geterotsiklicheskikh Soedinenii 10 (1981) 1299.
[5] P.N. Gaponik, S.V. Voitekhovich, O.A. Ivashkevich, Russian Chemical Reviews 75 (2006) 507.
[6] J. Stierstorfer, K.R. Tarantik, T.M. Klapötke, Chemistry - A European Journal 15 (2009) 5775.
[7] B.C.H. May, A.D. Abell, Journal of the Chemical Society - Perkin Transactions 1 (2002) 172.
[8] W.C. McCrone, D. Grabar, E. Lieber, Analytical Chemistry 23 (1951) 543.
[9] N. van der Putten, D. Heijdenrijk, H. Schenk, Acta Crystallographica Section C: Crystal Structure Communications 3 (1974) 321.
[10] R. Goddard, O. Heinemann, C. Krüger, Acta Crystallographica Section C: Crystal Structure Communications 53 (1997) 590.
[11] R.N. Butler, V.C. Garvin, H. Lumbroso, C. Liègeois, Journal of the Chemical Society - Perkin Transactions 2 (1984) 721.
[12] C. Zhaoxu, X. Heming, Journal of Molecular Structure: THEOCHEM 453 (1998) 65.
[13] S.C.S. Bugalho, E.M.S. Macoas, M.L.S. Cristiano, R. Fausto, Physical Chemistry Chemical Physics 3 (2001) 3541.
[14] W.D. Krugh, L.P. Gold, Journal of Molecular Spectroscopy 49 (1974) 423.
[15] A. Razynska, A. Tempczyk, E. Malinski, J. Szafranek, Z. Grzonka, P. Hermann, Journal of the Chemical Society - Perkin Transactions 2 (1983) 379.
[16] M.H. Palmer, I. Simpson, J.R. Wheeler, Zeitschrift für Naturforschung A, A Journal of Physical Sciences 36 (1981) 1246.
[17] A. Gómez-Zavaglia, I.D. Reva, L. Frija, M.L. Cristiano, R. Fausto, Journal of Physical Chemistry A 109 (2005) 7967.
[18] A. Gómez-Zavaglia, I.D. Reva, L. Frija, M.L. Cristiano, R. Fausto, Journal of Molecular Structure 786 (2006) 182.
[19] G. Maier, J. Eckwert, A. Bothur, H.P. Reisenauer, C. Schmidt, Liebigs Annalen der Chemie (1996) 1041.
[20] L.M.T. Frija, I.V. Khmelinskii, M.L.S. Cristiano, Journal Organic Chemistry 71 (2006) 3583.
[21] L.M.T. Frija, I.V. Khmelinskii, I.D. Reva, C. Serpa, R. Fausto, M.L.S. Cristiano, Organic & Biomolecular Chemistry 6 (2008) 1046.
[22] A. Gómez-Zavaglia, I.D. Reva, L. Frija, M.L. Cristiano, R. Fausto, Journal of Photochemistry and Photobiology A, Chemistry 179 (2006) 243.
[23] A. Gómez-Zavaglia, I.D. Reva, L. Frija, M.L. Cristiano, R. Fausto, Journal of Photochemistry and Photobiology A Chemistry 180 (2006) 175.

[24] L.M.T. Frija, I.D. Reva, A. Gómez-Zavaglia, M.L.S. Cristiano, R. Fausto, Photochemical & Photobiological Sciences 6 (2007) 1170.
[25] L.M.T. Frija, I.D. Reva, A. Gómez-Zavaglia, M.L.S. Cristiano, R. Fausto, Journal of Physical Chemistry A 111 (2007) 2879.
[26] A. Ismael, M.L.S. Cristiano, R. Fausto, A. Gomez-Zavaglia, Journal of Physical Chemistry A 114 (2010) 13076.
[27] A. Ismael, A. Borba, L. Duarte, M. Giuliano, A. Gómez-Zavaglia, M.L.S. Cristiano, Journal of Molecular Structure 1025 (2012) 105.
[28] I.R. Dunkin, Spectrochimica Acta Part A: Molecular and Biomolecular Spectroscopy 42 (1986) 649.
[29] I.R. Dunkin, C.J. Shields, H. Quast, Tetrahedron 45 (1989) 259.
[30] A. Awadallah, K. Kowski, P. Rademacher, Journal of Heterocyclic Chemistry 34 (1997) 113.
[31] L.M.T. Frija, A. Ismael, M.L.S. Cristiano, Molecules 15 (5) (2010) 3757.
[32] T. Bally, Matrix isolation, in: R.A. Moss, M.S. Platz, J. Maitland Jones (Eds.), Reactive Intermediate Chemistry, WILEY, New York, 2004, pp. 797–846 (Chapter 17).
[33] E. Whittle, D.A. Dows, G.C. Pimentel, Journal of Chemical Physics 22 (1954) 1943;
E.D. Becker, G.C. Pimentel, Journal of Chemical Physics 25 (1956) 224.
[34] R.S. Sheridan, in: A. Padwa (Ed.), Organic Photochemistry, vol. 8, Marcel Dekker Inc., New York, 1987, pp. 159–248.
[35] I.R. Dunkin, Chemical Society Reviews 9 (1980) 1.
[36] N. Kus, A. Sharma, I. Reva, L. Lapinski, R. Fausto, Journal of Chemical Physics 136 (2012) 144509.
[37] L.M.T. Frija, R. Fausto, R.M.S. Loureiro, M.L.S. Cristiano, Journal of Molecular Catalysis A: Chemical 3015 (2009) 142.
[38] I.D. Reva, S.G. Stepanian, L. Adamowicz, R. Fausto, Chemical Physics Letters 374 (2003) 631.
[39] I.D. Reva, A.J. Lopes Jesus, M.T.S. Rosado, R. Fausto, M.E. Eusébio, J.S. Redinha, Physical Chemistry Chemical Physics 8 (2006) 5339.
[40] M.T.S. Rosado, A.J.L. Jesus, I.D. Reva, R. Fausto, J.S. Redinha, Journal of Physical Chemistry A 133 (2009) 7499.
[41] M. Pagacz-Kostrzewa, I.D. Reva, R. Bronisz, B.M. Giuliano, R. Fausto, M. Wierzejewska, Journal of Physical Chemistry A 115 (2011) 5693.
[42] A. Borba, A. Gómez-Zavaglia, P.N.N.L. Simões, R. Fausto, Journal of Physical Chemistry A 109 (2005) 3578.
[43] K.A. Jensen, M. Due, A. Holm, Acta Chemica Scandinavica 19 (1965) 438.
[44] D. Martin, W. Mucke, Chemische Berichte-Recueil 98 (1965) 2059.
[45] T. Pasinszki, N.P.C. Westwood, Journal of Physical Chemistry 99 (1995) 1649.
[46] V.I. Faustov, E.G. Baskir, A.A. Biryukov, Russian Chemical Bulletin 52 (2003) 2328.
[47] O.L. Chapman, J.-P. Le Roux, Journal of American Chemical Society 100 (1978) 282.
[48] J.C. Hayes, R.S. Sheridan, Journal of American Chemical Society 112 (1990) 5879.
[49] D. Martin, Tetrahedron Letters 5 (1964) 2829.
[50] D. Martin, A. Weise, Chemische Berichte-Recueil 99 (1966) 976.
[51] A. Holm, E. Hugejens, Acta Chemica Scandinavica, Series. B: Organic Chemistry and Biochemistry 28 (1974) 705.
[52] H. Fischer, S. Zeuner, K. Ackermann, U. Schubert, Journal of Organometallic Chemistry 263 (1984) 201.
[53] R.S. Eachus, A.A. Muenter, T.D. Pawlik, J.R. Lenhard, Journal of Physical Chemistry B 109 (2005) 10126.
[54] J.W. Taylor, Y. Jiang, D.R. Bassett, The use of carbodiimide chemistry in photolithography, in: Polymeric Materials Science & Engineering, 1991, pp. 50.
[55] T. Uchihara, T. Kamiya, S. Maedomari, M. Ganeko, S. Kinjo, Y. Tamaki, A. Kinjo, Journal of Photochemistry and Photobiology A: Chemistry 130 (2000) 63.
[56] S. Otsuka, A. Nakamura, T. Yoshida, Journal of Organometallic Chemistry 7 (1967) 339.
[57] R. Huisgen, D. Vossius, M. Appl, Chemische Berichte-Recueil 91 (1958) 1.
[58] R. Huisgen, M. Appl, Chemische Berichte-Recueil 91 (1958) 12.
[59] H.-J. Himmel, M. Junker, H. Schnöckel, Journal of Chemical Physics 117 (2002) 3321.
[60] L.M.T. Frija, I.V. Khmelinskii, M.L.S. Cristiano, Tetrahedron Letters 46 (2005) 6757.
[61] A. Ismael, C. Serpa, M.L.S. Cristiano, Photochemical & Photobiological Sciences 12 (2) (2013) 272.
[62] M.L.S. Cristiano, R.A.W. Johnstone, Journal of the Chemical Society - Perkin Transactions 2 (1997) 489.
[63] M.L.S. Cristiano, R.A.W. Johnstone, Journal of Chemical Research (1997) S164.
[64] J.V. Barkley, M.L.S. Cristiano, R.A.W. Johnstone, R.M.S. Loureiro, Acta Crystallographica C53 (1997) 383.
[65] N.C. Araújo, P.M.M. Barroca, A.F. Brigas, M.L.S. Cristiano, R.A.W. Jonhstone, R.M.S. Loureiro, P.C.A. Pena, Journal of the Chemical Society - Perkin Transactions 2 (9) (2002) 1213.
[66] L.M.T. Frija, I. Reva, A. Ismael, D.V. Coelho, R. Fausto, M.L.S. Cristiano, Organic & Biomolecular Chemistry 9 (2011) 6040.
[67] A. Kumar, D.C. Dittmer, Journal of Organic Chemistry 59 (1994) 4760.
[68] W. Adam, K. Peters, M. Renz, Angewandte Chemie International Edition 33 (1994) 1107.
[69] S.C. Bergmeier, D.M. Stanchina, Tetrahedron Letters 36 (1995) 4533.
[70] H. Quast, U. Nahr, Chemische Berichte-Recueil 118 (1985) 526.
[71] M. Pagacz-Kostrzewa, M. Mucha, M. Weselski, M. Wierzejewska, Journal of Photochemistry and Photobiology A: Chemistry 251 (2013) 118.
[72] H. Zhao, Z.-R. Qu, H.-Y. Ye, R.-G. Xiong, Chemical Society Reviews 37 (2008) 84.
[73] M. Pagacz-Kostrzewa, J. Krupa, A. Olbert-Majkut, M. Podruczna, R. Bronisz, M. Wierzejewska, Tetrahedron 67 (2011) 8572.
[74] A. Gómez-Zavaglia, A. Ismael, L.I.L. Cabral, A. Kaczor, J.A. Paixão, R. Fausto, M.L.S. Cristiano, Journal of Molecular Structure 1003 (2011) 103.
[75] A. Ismael, J.A. Paixão, R. Fausto, M.L.S. Cristiano, Journal of Molecular Structure 1023 (2012) 128.
[76] A. Ismael, A. Gómez-Zavaglia, A. Borba, M.L.S. Cristiano, R. Fausto, Journal of Physical Chemistry A 117 (2013) 3190.
[77] I. Reva, B.J.A.N. Almeida, L. Lapinski, R. Fausto, Journal of Molecular Structure 1025 (2012) 74.
[78] G.I. Yranzo, J. Elguero, R. Flammang, C. Wentrup, European Journal of Organic Chemistry 12 (2001) 2209.
[79] E.J. Baran, V.T. Yilmaz, Coordination Chemistry Reviews 250 (2006) 1980.
[80] D. Döpp, International Journal of Photoenergy 3 (2001) 41.
[81] D.W. Cho, S.W. Oh, D.U. Kim, H.J. Park, J.Y. Xue, U.C. Yoon, P.S. Mariano, Bulletin of the Korean Chemical Society 31 (2010) 2453.
[82] L. Duarte, I. Reva, M.L.S. Cristiano, R. Fausto, Journal of Organic Chemistry 78 (2013) 3271.